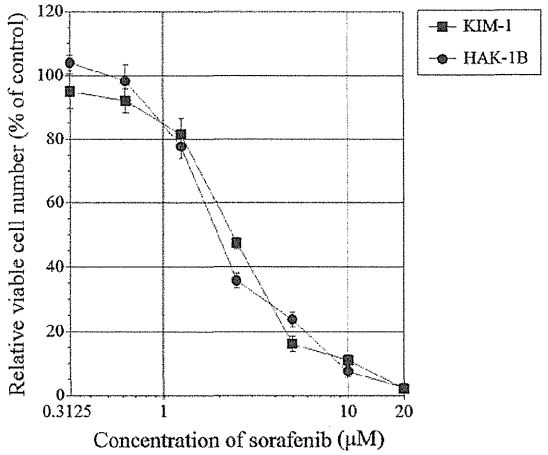

Figure 1. Seventy-two hours after adding 0.3125, 0.625, 1.25, 2.5, 5, 10 or 20 μM of sorafenib. Cell proliferation was suppressed in a dose-dependent manner in both KIM-1 and HAK-1B cell lines. The suppression was significant ($P<0.001$-0.05) in the range of 0.625-20 μM of sorafenib in KIM-1, 1.25-20 μM in HAK-1B. A total of 50% growth inhibitory dose was 2.5 μM in KIM-1 and 2.1 μM in HAK-1B. The values represent mean ± SD.

performed on the Discovery XT automated staining system (Ventana Medical Systems, Tucson, AZ, USA) to detect the apoptotic cells. This automated system uses the streptavidin-biotin complex method with DAB as a chromogen (Ventana iView DAB detection kit).

Microvessel density (MVD) was evaluated within the tumor according to a modified method introduced by Tanigawa *et al* (24). Briefly the slides stained with CD34 were screened at low power field (x40 or x100) and the two or three most vascular areas were selected. Microvessel counts of these areas were performed at high power field (x200, 0.74 mm^2). All positive stained cells were counted as microvessels and every 40 μm length of vessel lumen was calculated as one point. The average microvessel counts of selected areas were regarded as MVD, which was expressed as the absolute number of microvessels per 0.74 mm^2. Immunohistochemically, cleaved caspase-3 was expressed perinuclearly and Ki67 was on the nuclear. The rate of apoptotic cells and Ki67 labeling index were evaluated by calculating the rate of cleaved caspase-3-positive cells and Ki67-positive cells, respectively.

Statistical analysis. Comparisons of estimated tumor volume and colorimetric cell growth were performed using two-factor factorial ANOVA and Student's t-test, respectively. The other data comparisons were performed using the Mann-Whitney U test.

Results

Effect of sorafenib alone or combination treatment of sorafenib and PEG-IFN-α2b on the proliferation of HAK-1B or KIM-1 HCC cells in vitro. Seventy-two hours after the addition of sorafenib, the relative viable cell number was suppressed in both HAK-1B and KIM-1 cell lines in a dose-dependent manner (Fig. 1). The 50% inhibitory concentration (IC_{50}) was 2.1 μM for HAK-1B and 2.5 μM for KIM-1.

Seventy-two hours after the addition of PEG-IFN-α2b and sorafenib, the relative viable cell number was suppressed to various degrees. The results are shown in Fig. 2. In HAK-1B cell line (Fig. 2A), significant difference in the relative viable cell number was observed between combination group and sorafenib or PEG-IFN-α2b alone groups, additionally, CI in all combination of PEG-IFN-α2b and sorafenib was <0.9. The CI was 0.879 in the combination of 2,000 IU/ml of PEG-IFN-α2b and

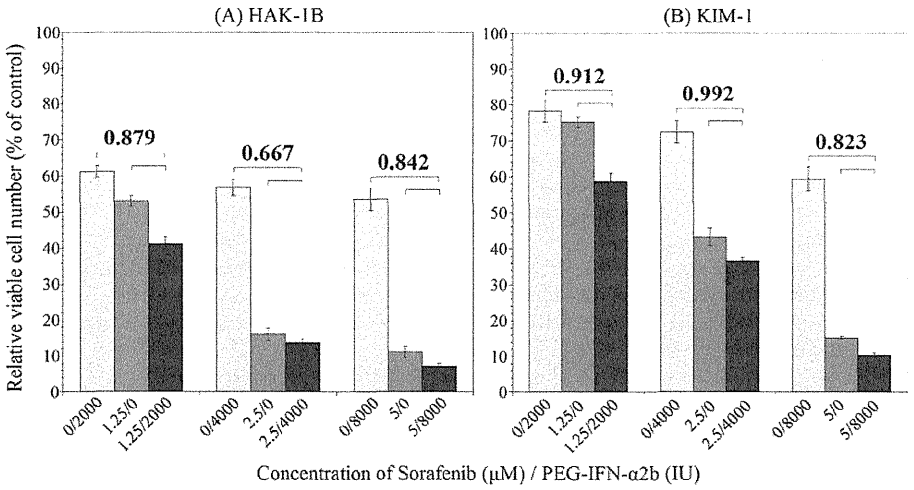

Figure 2. Effect of PEG-IFN-α2b and/or sorafenib on the proliferation of human HCC cell lines (A) HAK-1B and (B) KIM-1 in culture for 72 hours. Light gray bars are PEG-IFN-α2b alone group, dark gray bars sorafenib alone group, and black bars PEG-IFN-α2b + sorafenib group. All combination groups showed significant difference compared with monotherapy groups. The numbers above bars are CI. A CI of 0.9-1.1 indicates a nearly additive effect, a CI of <0.9 a synergistic effect, a CI of >1.1 an antagonistic effect. Representative data of two independent experiments are shown. The values represent mean ± SD.

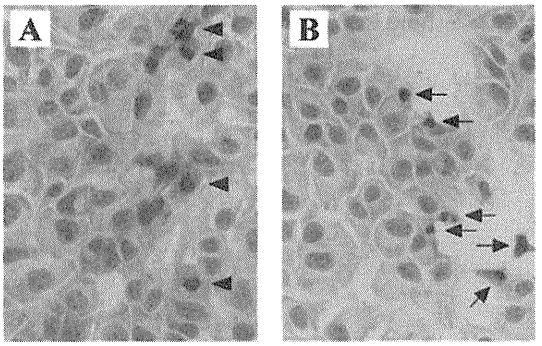

Figure 3. Photomicrograph of HAK-1B cells cultured for 72 h on Lab-Tek Chamber slide. (A) Without sorafenib in culture medium. Some mitotic figures were noted (arrowheads). (B) With 1.25 μM of sorafenib in culture medium. There were some apoptotic cells characterized by cytoplasmic shrinkage and nuclear chromatin condensation (arrows).

1.25 μM of sorafenib, 0.667 in 4,000 IU/ml of PEG-IFN-α2b and 2.5 μM of sorafenib, and 0.842 in 8,000 IU/ml of PEG-IFN-α2b and 5.0 μM of sorafenib. According to the definition of the CI, these results indicate that a combination of PEG-IFN-α2b and sorafenib may produce a synergistic growth inhibitory effect in HAK-1B cell line. In KIM-1 cell line (Fig. 2B), there was also a significant difference in the relative viable cell numbers between combination group and monotherapy groups. The CI was 0.912 in the combination of 2,000 IU/ml of PEG-IFN-α2b and 1.25 μM of sorafenib, 0.992 in 4,000 IU/ml of PEG-IFN-α2b and 2.5 μM of sorafenib, and 0.823 in 8,000 IU/ml of PEG-IFN-α2b and 5.0 M of sorafenib. These results indicate that combination therapy may produce an additive or synergistic growth inhibitory effect in KIM-1 cell line.

Morphologically, HAK-1B cells showed characteristic features of apoptosis, such as cytoplasmic shrinkage and nuclear chromatin condensation at 72 h after adding 1.25 μM of sorafenib (Fig. 3).

Table I. The weight of subcutaneous tumors of HAK-1B cells or KIM-1 cells in nude mice at sacrifice.

	Tumor weight (g)	
Treatment group	HAK-1B	KIM-1
Control	0.333±0.03	0.504±0.17
PEG-IFN-α2b alone	0.078±0.02[a]	0.379±0.18
Sorafenib alone	0.236±0.06	0.206±0.04[c]
PEG-IFN-α2b + sorafenib	0.113±0.04[b]	0.185±0.12[c]

Tumor weight represents mean ± SE (g). [a]P<0.0001 vs. control, P<0.05 vs. sorafenib alone. [b]P<0.001 vs. control. [c]P<0.05 vs. control.

The rate of Annexin V-EGFP positive apoptotic cells was increased by adding 2 μM of sorafenib in HAK-1B cells (5.8% of the control and 37.8% of the sorafenib). In KIM-1 cells, however, the increase was relatively small (7.9% of the control and 9.5% of the sorafenib) (Fig. 4A). In another setting, the combination group with PEG-IFN-α2b showed higher rate of apoptosis than control or monotherapy groups in HAK-1B (4.8% of control, 37.4% of the PEG-IFN-α2b, 14.3% of the sorafenib, 42.8% of the combination) (Fig. 4B).

Effects of sorafenib and/or PEG-IFN-α2b on HAK-1B or KIM-1 cell proliferation in nude mice. Chronological changes in estimated tumor volume after subcutaneous injection of cultured HAK-1B cells or KIM-1 cells to nude mice are summarized in Fig. 5. The actual tumor weights at the time of sacrifice are shown in Table I. In the experiment of HAK-1B tumors, the tumor volume of mice receiving PEG-IFN-α2b, sorafenib, and sorafenib+PEG-IFN-α2b was 34, 73 and 36%, respectively, of the control volume and the tumor weight was 23, 71 and 34%, respectively, of the control weight. Statistically, there were significant differences both in tumor volume and weight

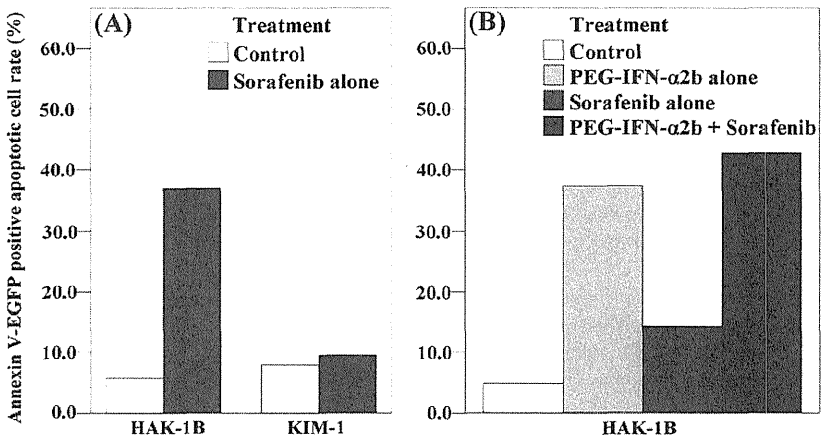

Figure 4. Quantitative analysis of Annexin V-EGFP positive apoptotic cells. (A) Apoptosis of HAK-1B or KIM-1 cells induced by 2 μM of sorafenib. (B) Apoptosis of HAK-1B cells induced by 2,000 IU/ml of PEG-IFN-α2b and/or 1.25 M of sorafenib. Representative data of three independent experiments are shown.

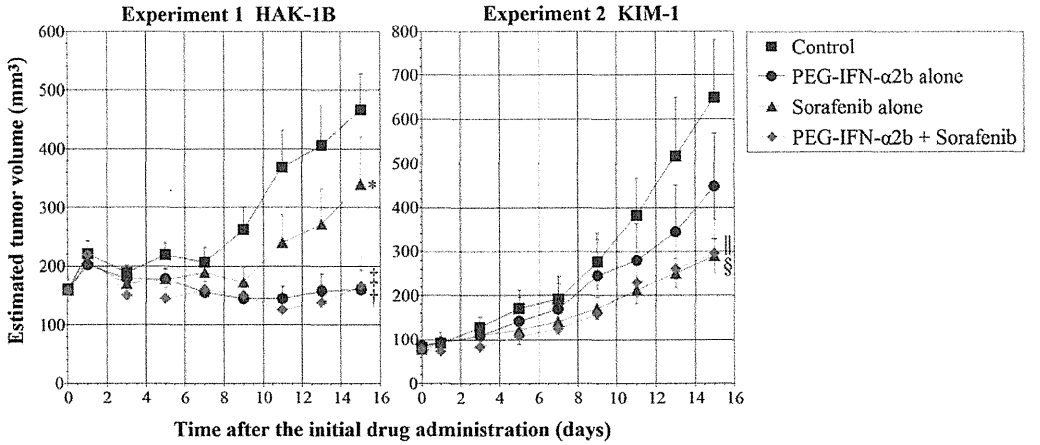

Figure 5. Chronological changes on the estimated volume of HAK-1B (Experiment 1) or KIM-1 (Experiment 2) tumor that was developed subcutaneously on nude mice. The PEG-IFN-α2b alone group (●) received subcutaneous injection of 1,920 IU twice a week for 14 days. The sorafenib alone group (▲) received 10 mg/kg/mouse/day orally every day for 14 days. The PEG-IFN-α2b + sorafenib group (◆) received 1,920 IU of PEG-IFN-α2b twice a week and 10 mg/kg of sorafenib every day for 14 days. The control group (■) received subcutaneous injection of 0.1 ml of medium twice a week and 0.2 ml of Cremophor EL/ethanol/water (12.5/12.5/75). The values represent mean ± SE. *P<0.05 vs. control. †P<0.0001 vs. control, P<0.005 vs. sorafenib alone. ‡P<0.0001 vs. control, P<0.001 vs. sorafenib alone. §P<0.001 vs. control. ‖P<0.0001 vs. control.

Table II. MVD and the ratio of apoptotic cells and Ki67 positive cells in human HCC tumors subcutaneously transplanted in nude mice.

Cell line	Treatment group	MVD	Apoptotic cells	Ki67 positive cells
HAK-1B	Control	100.8±7.7	3.8±0.4	36.8±2.0
	Peg-IFN-α2b alone	114.9±16.7	4.4±0.4	37.5±4.6
	Sorafenib alone	53.8±4.3[a]	6.7±1.3[b]	38.3±2.0
	Peg-IFN-α2b + soragfenib	69.4±10.1[b]	5.6±1.3[b]	35.3±2.2
KIM-1	Control	125.9±16.2	4.6±0.4	6.7±0.2
	Peg-IFN-α2b alone	97.4±10.4	5.1±0.4	7.5±0.8
	Sorafenib alone	85.1±6.6[b]	6.5±0.7[b]	5.7±0.4
	Peg-IFN-α2b + soragfenib	79.0±7.2[b]	6.3±0.6[b]	4.6±0.5[c]

Scores represent mean ± SE. [a]P<0.0005 vs. control, P<0.01 vs. Peg-IFN-α2b alone. [b]P<0.05 vs. control. [c]P<0.005 vs. control, P<0.05 vs. Peg-IFN-α2b alone.

between the control group and the PEG-IFN-α2b alone group (P<0.0001 vs. control in tumor volume, P<0.0001 vs. control in tumor weight) or the combination group (P<0.0001 vs. control in tumor volume, P<0.001 vs. control in tumor weight) and between the sorafenib alone group and the PEG-IFN-α2b alone group (P<0.005 vs. sorafenib alone in tumor volume, P<0.05 vs. sorafenib alone in tumor weight). Although there was a significant difference between the sorafenib alone group and the combination group in tumor volume (P<0.001), this was not the case in the actual tumor weight (P=0.099). In the experiment of KIM-1 tumors, the tumor volume of mice receiving PEG-IFN-α2b, sorafenib, and sorafenib+PEG-IFN-α2b was 69, 45 and 46%, respectively, of the control volume and the tumor weight was 75, 41 and 37%, respectively, of the control weight. Statistically, there were significant differences in both tumor volume and weight between the control and the sorafenib alone group (P<0.0001 vs. control in tumor volume, P<0.05 vs. control in tumor weight) or the combination group (P<0.001 vs. control in tumor volume, P<0.05 vs. control in tumor weight).

The results of immunohistochemical examination are summarized in Table II. The significant decrease of MVD and increase of apoptotic cells were observed in the sorafenib group (P<0.0005 and 0.05 respectively vs. control in HAK-1B, P<0.05 and 0.05 respectively vs. control in KIM-1) and the combination group (P<0.05 and 0.05 respectively vs. control in HAK-1B, P<0.05 and 0.05, respectively, vs. control in KIM-1) compared to the control group in both HAK-1B and KIM-1 tumors, although there was no significant difference between the combination group and monotherapy groups. Ki67 labeling index was significantly lower in the combination group (P<0.005 vs. control, P<0.05 vs. PEG-IFN-α2b group) than in the control group or the PEG-IFN-α2b group only in KIM-1.

Discussion

In this study, we showed the synergistic effect of sorafenib and PEG-IFN-α2b on HAK-1B cells *in vitro*. We previously reported that PEG-IFN-α2b induced apoptosis on both HAK-1B and KIM-1 cells *in vitro* (14). We found that sorafenib also induced apoptosis on HAK-1B *in vitro*. On the other hand, the increase of apoptotic cells was not clearly observed on KIM-1 cells in spite of the fact that the proliferation of KIM-1 cells was inhibited by sorafenib in MTT assay. A possible explanation is that cell proliferation might be inhibited by other antiproliferative mechanisms. The blockade of Raf signaling which is the main effect of sorafenib can lead to the repression of transforming growth factor α-epidermal growth factor receptor autocrine loops of tumor cells (5). Such a mechanism could have inhibited the growth of KIM-1 cells. In addition, a limitation of *in vitro* study is that we are not able to assess the indirect anti-angiogenic effect against endothelial cells.

In the *in vivo* study, there was a significant reduction of tumor volume and weight in the combination group on both HAK-1B and KIM-1 tumors compared with the control group. However, there was no significant difference between the combination and the monotherapy groups, and it seemed that HAK-1B tumors were sensitive to PEG-IFN-α2b and KIM-1 tumors to sorafenib. Only in KIM-1 tumors that might be sensitive to sorafenib, Ki67 labeling index was lower in the combination group than in the control group. Recently Wang *et al* (25) reported that combination therapy of sorafenib with recombinant human INF-α2a was effective *in vitro* and *in vivo* on two HCC cell lines, Huh-7 and Sk-Hep-1. In their study, the significant differences between combination and monotherapy groups were clearly observed. This partial difference might be due to the different experimental settings, such as different cell lines and different dose of drugs. One of the greatest differences, we surmise, is the site of IFN administration. They injected IFN directly into subcutaneous tumors, whereas we did subcutaneously but not into the tumors.

Since sorafenib is a multikinase inhibitor, it is considered that sorafenib has both direct antiproliferative effect due to the blockade of Raf kinase on tumor cells themselves and indirect effect due to the blockade of receptor tyrosine kinases, such as VEGFR-2, on endothelial cells followed by the inhibition of angiogenesis (5). Therefore we also evaluated MVD of xenografts and confirmed the significant decrease of MVD in the sorafenib alone and the combination group in both HAK-1B and KIM-1 tumors. It has been repeatedly shown that IFN suppresses the growth of various types of human tumors that were transplanted into mice through the anti-angiogenic effect. Tedjarati *et al* (26) reported that the subcutaneous injection of 7,000 IU per week of PEG-IFN-α2b into nude mice bearing human ovarian cancer cells induced a significant decrease of CD31-positive endothelial cells and Huang *et al* (27) showed similar results with the subcutaneous injection of 70,000 IU per week of PEG-IFN-α2b on human prostate cancer cells. PEG-IFN-α2b administered at higher or lower doses was less effective. In our current study, however, there was no significant decrease of MVD in the PEG-IFN-α2b group compared with the control group. Moreover, in our previous report, the decrease of artery-like blood vessels was not observed in the same HAK-1B tumors by the administration of PEG-IFN-α2b at either higher or lower doses (14).

Another notable finding regarding the MVD in this study is the discrepancy between MVD and tumor weight or size. Interestingly, the reduction of tumor weight and size was not so much in sorafenib monotherapy group in HAK-1B tumors despite the most prominent decrease of MVD was observed in this group. On the other hand, there was a significant reduction of tumor weight and size in PEG-IFN-α2b alone group in HAK-1B, although this group did not show any significant decrease of MVD. This result supports our previous findings in which we showed there was no relationship between tumor shrinkage and the number of artery-like blood vessels in HAK-1B tumors after the administration of the various concentration of PEG-IFN-α2b (14). Hlatky *et al* (28) mentioned in their review article that the efficacy of anti-angiogenic agents cannot be simply visualized by alterations in microvessel density during treatment because of the difference of the tightness of the coupling between vessel drop-out and tumor-cell drop-out after the treatment. In addition, Yao *et al* (29) recently reported that the expression of VEGFR-1 in tumor cells which is normally expressed specifically in endothelial cells were strongly associated with anti-PlGF antibody efficacy, but not with anti-angiogenesis. More studies are needed to investigate new approaches to assess the efficacy of anti-angiogenic drugs *in vivo* and molecular mechanisms of their action of 'anti-angiogenic' drugs.

In conclusion, we demonstrated the synergistic antiproliferative effect of combination therapy on HAK-1B cells *in vitro*. Although, *in vivo* the synergistic effects of the combination therapy were not clearly observed, the combination therapy induced nearly maximal antitumor effects, independent of the HCC cell sensitivity to antitumor effects of single therapy with either PEG-IFN-α2b or sorafenib. These findings suggest that PEG-IFN-α2b might be a promising candidate for use in combination therapy with sorafenib and warrant further investigation.

Acknowledgements

We are grateful to Ms. Akemi Fujiyoshi and Ms. Sachiyo Maeda for their excellent technical assistance. This study was supported in part by grant-in-aid from Ministry of Health, Labor and Welfare of Japan.

References

1. Ferlay J, Shin H-R, Bray F, Forman D, Mathers C and Parkin DM: Estimates of worldwide burden of cancer in 2008: GLOBOCAN 2008. Int J Cancer 127: 2893-2917, 2008.
2. Llovet JM, Burroughs A and Bruix J: Hepatocellular carcinoma. Lancet 362: 1907-1917, 2003.
3. Bruix J and Sherman M: Management of hepatocellular carcinoma. Hepatology 42: 1208-1236, 2005.
4. Llovet JM, Bustamante J, Castells A, Vilana R, Ayuso Mdel C, Sala M, Brú C, Rodés J and Bruix J: Natural history of untreated nonsurgical hepatocellular carcinoma: rationale for the design and evaluation of therapeutic trials. Hepatology 29: 62-67, 1999.
5. Wilhelm SM, Adnane L, Newell P, Villanueva A, Llovet JM and Lynch M: Preclinical overview of sorafenib, a multikinase inhibitor that targets both Raf and VEGF and PDGF receptor tyrosine kinase signaling. Mol Cancer Ther 7: 3129-3140, 2008.

6. Llovet JM, Ricci S, Mazzaferro V, Hilgard P, Gane E, Blanc JF, de Oliveira AC, Santoro A, Raoul JL, Forner A, Schwartz M, Porta C, Zeuzem S, Bolondi L, Greten TF, Galle PR, Seitz JF, Borbath I, Häussinger D, Giannaris T, Shan M, Moscovici M, Voliotis D and Bruix J; SHARP Investigators Study Group: Sorafenib in advanced hepatocellular carcinoma. N Engl J Med 359: 378-390, 2008.
7. Cheng AL, Kang YK, Chen Z, Tsao CJ, Qin S, Kim JS, Luo R, Feng J, Ye S, Yang TS, Xu J, Sun Y, Liang H, Liu J, Wang J, Tak WY, Pan H, Burock K, Zou J, Voliotis D and Guan Z: Efficacy and safety of sorafenib in patients in the Asia-Pacific region with advanced hepatocellular carcinoma: a phase III randomised, double-blind, placebo-controlled trial. Lancet Oncol 10: 25-34, 2009.
8. Gollob JA, Rathmell WK, Richmond TM, Marino CB, Miller EK, Grigson G, Watkins C, Gu L, Peterson BL and Wright JJ: Phase II trial of sorafenib plus interferon alfa-2b as first- or second-line therapy in patients with metastatic renal cell cancer. J Clin Oncol 25: 3288-3295, 2007.
9. Escudier B, Szczylik C, Hutson TE, Demkow T, Staehler M, Rolland F, Negrier S, Laferriere N, Scheuring UJ, Cella D, Shah S and Bukowski RM: Randomized phase II trial of first-line treatment with sorafenib versus interferon alfa-2a in patients with metastatic renal cell carcinoma. J Clin Oncol 27: 1280-1289, 2009.
10. Sakon M, Nagano H, Dono K, Nakamori S, Umeshita K, Yamada A, Kawata S, Imai Y, Iijima S and Monden M: Combined intraarterial 5-fluorouracil and subcutaneous interferon-α therapy for advanced hepatocellular carcinoma with tumor thrombi in the major portal branches. Cancer 94: 435-442, 2002.
11. Pestka S, Langer JA, Zoon KC and Samuel CE: Interferons and their actions. Annu Rev Biochem 56: 727-777, 1987.
12. Yano H, Iemura A, Haramaki M, Ogasawara S, Takayama A, Akiba J and Kojiro M: Interferon alfa receptor expression and growth inhibition by interferon alfa in human liver cancer cell lines. Hepatology 29: 1708-1717, 1999.
13. Hisaka T, Yano H, Ogasawara S, Momosaki S, Nishida N, Takemoto Y, Kojiro S, Katafuchi Y and Kojiro M: Interferon-αCon1 suppresses proliferation of liver cancer cell lines in vitro and in vivo. J Hepatol 41: 782-789, 2004.
14. Yano H, Ogasawara S, Momosaki S, Akiba J, Kojiro S, Fukahori S, Ishizaki H, Kuratomi K, Basaki Y, Oie S, Kuwano M and Kojiro M: Growth inhibitory effects of pegylated IFN alpha-2b on human liver cancer cells in vitro and in vivo. Liver Int 26: 964-975, 2006.
15. Ikeda K, Saitoh S, Arase Y, Chayama K, Suzuki Y, Kobayashi M, Tsubota A, Nakamura I, Murashima N, Kumada H and Kawanishi M: Effect of interferon therapy on hepatocellular carcinogenesis in patients with chronic hepatitis type C: a long-term observation study of 1643 patients using statistical bias correction with proportional hazard analysis. Hepatology 29: 1124-1130, 1999.
16. Ikeda K, Arase Y, Saitoh S, Kobayashi M, Suzuki Y, Suzuki F, Tsubota A, Chayama K, Murashima N and Kumada H: Interferon beta prevents recurrence of hepatocellular carcinoma after complete resection or ablation of the primary tumor-A prospective randomized study of hepatitis C virus-related liver cancer. Hepatology 32: 228-232, 2000.
17. Mazzella G, Accogli E, Sottili S, Festi D, Orsini M, Salzetta A, Novelli V, Cipolla A, Fabbri C, Pezzoli A and Roda E: Alpha interferon treatment may prevent hepatocellular carcinoma in HCV-related liver cirrhosis. J Hepatol 24: 141-147, 1996.
18. Nishiguchi S, Kuroki T, Nakatani S, Morimoto H, Takeda T, Nakajima S, Shiomi S, Seki S, Kobayashi K and Otani S: Randomised trial of effects of interferon-α on incidence of hepatocellular carcinoma in chronic active hepatitis C with cirrhosis. Lancet 346: 1051-1055, 1995.
19. Nishiguchi S, Tamori A and Kubo S: Effect of long-term postoperative interferon therapy on intrahepatic recurrence and survival rate after resection of hepatitis C virus-related hepatocellular carcinoma. Intervirology 48: 71-75, 2005.
20. Sakaguchi Y, Kudo M, Fukunaga T, Minami Y, Chung H and Kawasaki T: Low-dose, long-term, intermittent interferon-alpha-2b therapy after radical treatment by radiofrequency ablation delays clinical recurrence in patients with hepatitis C virus-related hepatocellular carcinoma. Intervirology 48: 64-70, 2005.
21. Murakami T: Establishment and characterization of human hepatoma cell line (KIM-1). Acta Hepatol Jpn 25: 532-539, 1984.
22. Yano H, Iemura A, Fukuda K, Mizoguchi A, Haramaki M and Kojiro M: Establishment of two distinct human hepatocellular carcinoma cell lines from a single nodule showing clonal dedifferentiation of cancer cells. Hepatology 18: 320-327, 1993.
23. Chou TC and Talalay P: Quantitative analysis of dose-effect relationships: the combined effects of multiple drugs or enzyme inhibitors. Adv Enzyme Regul 22: 27-55, 1984.
24. Tanigawa N, Lu C, Mitsui T and Miura S: Quantification of sinusoid-like vessels in hepatocellular carcinoma: its clinical and prognostic significance. Hepatology 26: 1216-1223, 1997.
25. Wang L, Jia D, Duan F, Sun Z, Liu X, Zhou L, Sun L, Ren S, Ruan Y and Gu J: Combined anti-tumor effects of IFN-α and sorafenib on hepatocellular carcinoma in vitro and in vivo. Biochem Biophys Res Commun 422: 687-692, 2012.
26. Tedjarati S, Baker CH, Apte S, Huang S, Wolf JK, Killion JJ and Fidler IJ: Synergistic therapy of human ovarian carcinoma implanted orthotopically in nude mice by optimal biological dose of pegylated interferon alpha combined with paclitaxel. Clin Cancer Res 8: 2413-2422, 2002.
27. Huang SF, Kim SJ, Lee AT, Karashima T, Bucana C, Kedar D, Sweeney P, Mian B, Fan D, Shepherd D, Fidler IJ, Dinney CP and Killion JJ: Inhibition of growth and metastasis of orthotopic human prostate cancer in athymic mice by combination therapy with pegylated interferon-alpha-2b and docetaxel. Cancer Res 62: 5720-5726, 2002.
28. Hlatky L, Hahnfeldt P and Folkman J: Clinical application of antiangiogenic therapy: microvessel density, what it does and doesn't tell us. J Natl Cancer Inst 94: 883-893, 2002.
29. Yao J, Wu X, Zhuang G, Kasman IM, Vogt T, Phan V, Shibuya M, Ferrara N and Bais C: Expression of a functional VEGFR-1 in tumor cells is a major determinant of anti-PlGF antibodies efficacy. Proc Natl Acad Sci USA 108: 11590-11595, 2011.

OPEN ACCESS Freely available online

PLOS | ONE

Pegylated Interferon-α2a Inhibits Proliferation of Human Liver Cancer Cells *In Vitro* and *In Vivo*

Hironori Kusano[1*], Jun Akiba[1], Sachiko Ogasawara[1], Sakiko Sanada[1], Makiko Yasumoto[1], Masamichi Nakayama[1], Keiko Ueda[1], Kosuke Ueda[1], Takashi Kurita[1], Keita Todoroki[1], Yumi Umeno[1], Osamu Nakashima[2], Hirohisa Yano[1]

1 Department of Pathology, Kurume University School of Medicine, Kurume, Fukuoka, Japan, 2 Department of Clinical Laboratory Medicine, Kurume University Hospital, Kurume, Fukuoka, Japan

Abstract

Purpose: We investigated the effects of pegylated interferon-α2a (PEG-IFN-α2a) on the growth of human liver cancer cells.

Methods: The effect of PEG-IFN-α2a on the proliferation of 13 liver cancer cell lines was investigated *in vitro*. Cells were cultured with medium containing 0–4,194 ng/mL of PEG-IFN-α2a, and after 1, 2, 3, or 4 days of culture, morphologic observation and growth assay were performed. After hepatocellular carcinoma (HCC) cells (HAK-1B and KIM-1) were transplanted into nude mice, various doses of PEG-IFN-α2a were subcutaneously administered to the mice once a week for 2 weeks, and tumor volume, weight, and histology were examined.

Results: PEG-IFN-α2a inhibited the growth of 8 and 11 cell lines in a time- and dose-dependent manner, respectively, although the 50% growth inhibitory concentrations of 7 measurable cell lines on Day 4 were relatively high and ranged from 253 ng/mL to 4,431 ng/mL. Various levels of apoptosis induction were confirmed in 8 cell lines. PEG-IFN-α2a induced a dose-dependent decrease in tumor volume and weight, and a significant increase of apoptotic cells in the tumor. Subcutaneous administration of clinical dose for chronic hepatitis C (3 μg/kg, 0.06 μg/mouse) was effective and induced about 30-50% reduction in the tumor volume and weight as compared with the control.

Conclusions: Although *in vitro* anti-proliferative effects of PEG-IFN-α2a were relatively weak, PEG-IFN-α2a induced strong anti-tumor effects on HCC cells *in vivo*. The data suggest potential clinical application of PEG-IFN-α2a for the prevention and treatment of HCC.

Citation: Kusano H, Akiba J, Ogasawara S, Sanada S, Yasumoto M, et al. (2013) Pegylated Interferon-α2a Inhibits Proliferation of Human Liver Cancer Cells *In Vitro* and *In Vivo*. PLoS ONE 8(12): e83195. doi:10.1371/journal.pone.0083195

Editor: Diego Calvisi, Institut für Pathologie, Greifswald, Germany, Germany

Received August 19, 2013; **Accepted** November 10, 2013; **Published** December 12, 2013

Funding: This study was supported in part by the Sarah Cousins Memorial Fund, Boston, Massachusetts, and by a Grant-in-Aid from the Ministry of Health, Labor and Welfare of Japan. The funders had no role in study design, data collection and analysis, decision to publish, or preparation of the manuscript.

Competing interests: The authors have declared that no competing interests exist.

* E-mail: kusano_hironori@kurume-u.ac.jp

Introduction

Interferons (IFNs) are types of cytokine that are produced by host cells, such as leukocytes, in response to inflammation. Since IFNs possess antiviral activity, antiproliferative activity and various immunoregulatory activities, IFN therapy is used to treat patients with chronic viral hepatitis or certain types of cancer including malignant melanoma, acquired immunodeficiency syndrome-related Kaposi's sarcoma and some hematopoietic malignancies [1,2]. Lai et al also showed that recombinant IFNα is useful in prolonging survival among patients with inoperable hepatocellular carcinoma (HCC) [3]. In addition, some studies showed IFN therapy might prevent either occurrence or recurrence after initial curative therapy of HCC, such as liver resection and radiofrequency ablation, in patient with chronic viral hepatitis [4–7]. This cancer preventive effect of IFNs is regarded mainly as results of their antiviral effect and the consequent suppression of inflammation, and might be due to their direct antitumor effect against clinically undetectable HCC as well. The detailed mechanism of the antitumor effect of IFNs, however, remains obscure.

Pegylated interferon-α2a (PEG-IFN-α2a) and pegylated interferon-α2b (PEG-IFN-α2b), which are used to treat patients with chronic hepatitis C virus (HCV) or B virus (HBV) infection, are modified IFNs that have longer serum half-life in body than non-pegylated forms of IFNs, therefore they can be given to

patients only once a week, whereas a standard IFN without pegylation used to be injected up to three to five times a week. This once-a-week injection of pegylated IFNs in combination with daily oral dosing of the nucleoside analogue ribavirin has substantially improved the rate of sustained virological response in patients with chronic HCV infection and got a position as the first line therapy [8,9]. We previously reported that PEG-IFN-α2b which contains 12 kDa polyethylene glycol (PEG) has stronger antitumor effects *in vivo* than non-pegylated IFNs and this result might be indicating that continuous IFNs exposure to cancer cells in body is more effective than continual injection [10]. On the basis of above-described background, we examined the growth inhibitory effects of PEG-IFN-α2a which contains two chains of 20 kDa PEG and has the longest serum half-life among clinically available IFNs on liver cancer cell lines *in vitro* and *in vivo*.

Methods

Cell Lines and Cell Culture

This study used 11 HCC cell lines (KIM-1, KYN-1, KYN-2, KYN-3, HAK-1A, HAK-1B, HAK-2, HAK-3, HAK-4, HAK-5, and HAK-6) and 2 human combined hepatocellular and cholangiocarcinoma (CHC) cell lines (KMCH-1 and KMCH-2). These HCC and CHC cell lines were originally established in our laboratory, and each cell line retains the morphological and functional features of the original tumor as described elsewhere [11–20]. Since tumorigenicity is higher in HAK-1B and KIM-1 cells than in the other 11 cell lines that we have, we used these two cell lines for *in vivo* study.

The cells were grown in Dulbecco's Modified Eagle Medium (Nissui Seiyaku, Co., Japan) supplemented with 2.5% heat-inactivated (56°C, 30 min) fetal bovine serum (FBS, Bioserum, Victoria, Australia), 100 U/mL penicillin, 100 μg/mL streptomycin (GIBCO BRL/Life Technologies, Inc., Gaithersburg, MD) and 12 mmol/L sodium bicarbonate, in a humidified atmosphere of 5% CO_2 in air at 37°C.

IFN and Reagents

PEG-IFN-α2a (PEGASYS®, Chugai Pharmaceutical Co., Ltd., Tokyo, Japan) with the specific activity of 1.4 X 10^7 IU/mg protein and non-pegylated IFN-α2a (Miltenyi Biotec GmbH, Bergisch Gladbach, Germany) with that of 2.0 X 10^8 IU/mg protein were used in the study.

Anti-bromodeoxyuridine (BrdU) antibody and fluorescein isothiocyanate-conjugated goat anti-mouse immunoglobulin (FITC-GAM) were purchased from Becton Dickinson Immunocytometry Systems USA (San Jose, CA); control normal mouse IgG_1, from DAKO (Glostrup, Denmark); rat antibody against mouse endothelial cells (anti-CD34, clone MEC14.7), from Serotec Co., UK; and mouse monoclonal antibody against human α-smooth muscle actin (SMA) that cross-reacts with mouse α-SMA (clone 1A4).

Effects of PEG-IFN-α2a on the Proliferation of HCC and CHC Cell Lines *in vitro*

The effects of PEG-IFN-α2a on the growth of the cultured cells were examined with colorimetry using 3-(4,5-dimethylthiazol-2yl)-2,5-diphenyl tetrazolium bromide (MTT) assay kits (Chemicon, Temecula, CA) as described elsewhere [18,21]. Briefly, the cells (1.5~8 X 10^3 cells per well) were seeded on 96-well plates (Nunc, Inc, Roskilde, Denmark), cultured for 24 hours, and the culture medium was changed to a new medium with or without PEG-IFN-α2a (0.016, 0.064, 0.256, 1.024, 4.096, 16.4, 65.5, 262, 1,048, or 4,194 ng/mL). After culturing for 24, 48, 72 or 96 hours, the number of viable cells was measured with ImmunoMini NJ-2300 (Nalge Nunc International, Tokyo, Japan) by setting the test wavelength at 570 nm and the reference wavelength at 630 nm. To keep the optical density within linear range, all experiments were performed while the cells were in the logarithmic growth phase.

Quantitative analysis of apoptotic cells induced by PEG-IFN-α2a

HAK-1B or KIM-1 cells cultured with medium alone (control), non-pegylated IFN-α2a (10 ng/ml=2,000 IU/ml) or PEG-IFN-α2a (144 ng/ml=2,000 IU/ml) for 72 hours were stained with the Annexin V-EGFP (enhanced green fluorescent protein) Apoptosis Detection Kits (Medical & Biological Laboratories Co., Ltd.) according to the manufacturer's instructions. After staining, the cells were analyzed using a FACScan (Becton Dickinson Immunocytometry Systems, San Jose, CA), and Annexin V-EGFP-positive apoptotic cell rate was determined.

Morphological Observation

For morphological observation under a light microscope, cultured cells were seeded on Lab-Tek tissue culture chamber slides (Nunc, Inc.), cultured with or without PEG-IFN-α2a (262, 1,048 or 4,194 ng/mL) for 72 hours, fixed for 10 min in Carnoy's solution, and stained with hematoxylin-eosine (HE).

Effects of PEG-IFN-α2a on HCC Cell Proliferation in Nude Mice

All animal experiments were approved by the institutional committee for animal experiments in Kurume University School of Medicine (Permit Number: 1334), and conducted according to the Guide for the Care and Use of Laboratory Animals of the National Institute of Health and the Regulations for Animal Experimentation of Kurume University School of Medicine. Mice were killed by cervical dislocation under diethyl ether anesthesia, and all efforts were made to minimize suffering. Cultured HAK-1B or KIM-1 (10^7 cells/mouse) was subcutaneously (s.c.) injected into the backs of 5-week-old female BALB/c athymic nude mice (Clea Japan, Inc., Osaka, Japan). Five to seven days later when the largest diameter of the tumor, which was measured by using caliper, reached approximately 5~10 mm (Day 0), tumor volume (mm^3) was calculated in the equation 'the largest diameter X (the smallest diameter)^2 X 0.5', and then the mice were divided into 5 groups (n=8 each). Tumor volume was measured on Day 0, 1, 2, 4, 6, 8, 10, 12, and 14. Mouse body weight was measured on Day 0,

8, and 14. After 2-week treatment, mice were killed on Day 15 and the actual tumor weight was also measured. In experiment 1, the 5 groups of 8 mice received either phosphate-buffered saline (PBS) (Control) or PBS with the different dosages of PEG-IFN-α2a (0.06–60 μg) once a week for 2 consecutive weeks (Day 1 and Day 8). The clinical dose of PEG-IFN-α2a in chronic hepatitis C treatment is about 3 μg/kg and is equivalent to the lowest dose (0.06 μg/mouse=840 IU/mouse) in this experiment. After killing, resected tumors were used for morphological studies (e.g., HE staining and immunohistochemistry) and Enzyme-linked immunosorbent assay (ELISA) analysis. Every mouse received an intraperitoneal injection of 1 mg of BrdU 30 min before killing. In experiment 2, to examine the difference between non-pegylated and pegylated IFNs, 5 groups of 8 mice received either PBS (Control), PBS with 0.0042 or 0.042 μg of IFN-α2a (840 or 8,400 IU, respectively), or PBS with 0.06 or 0.6 μg of PEG-IFN-α2a (840 or 8,400 IU, respectively). In this experiment, tumor weights on Day 15 and numbers of apoptotic cells were compared among the groups.

Morphological Examination of the Subcutaneous Tumors of Nude Mice

The number of cells showing the characteristics of apoptosis (e.g., cytoplasmic shrinkage, chromatin condensation, and nuclear fragmentation) was counted in at least three 0.25 mm^2-areas within an HE-stained specimen, and the average number per area was obtained. The TUNEL technique (ApopTag® Peroxidase *In Situ* apoptosis Detection Kits, CHEMICON International, Inc, CA) was used to detect apoptotic cells, and the average number of TUNEL-positive cells per area was obtained, as described above. The specimens were also immunostained for incorporated BrdU using BrdU Staining Kits (Oncogene Research Products, Boston, MA), and the average number of positive cells per area was obtained as described above. In addition, double-immunostaining was performed with anti-mouse endothelial cell antibody, anti-human α-SMA antibody, Histofine simple stain mouse MAX-PO (Rat) kits (Nichirei, Tokyo, Japan), and HistoMouse™-plus kits to detect artery-like blood vessels as described in our previous report [21,22]. The number of double-immunostaining-positive blood vessels in the tumor was counted on each specimen. Granulation tissue within the tumor were excluded in counting of blood vessels. The size of the counted area was measured by tracing the outline displayed on a computer monitor using Mac SCOPE (MITANI Corp., Chiba, Japan). From the obtained number of vessels per unit area (mm^2), the group mean was obtained for group comparison.

Enzyme-linked immunosorbent assay (ELISA)

Portions of the resected xenograft tumors were homogenized in 500 μl of ice-cold Ca^{2+} and Mg^{2+}-free PBS containing 100 mg/ml phenymethylsulfonyl fluoride using a pellet pestle. The mixture was centrifuged for 10 min (12,000 g, 4°C), and the supernatant was stored at -20°C until use. After the determination of the amount of the tissue protein in the supernatant using a BCA protein assay reagent (Pierce, Rockford, IL), the amount of basic fibroblast growth factor (bFGF) and IL-8 was measured by using commercially available ELISA kits (R&D Systems, Minneapolis, MN).

Statistics

Comparisons of estimated tumor volume and colorimetric cell growth were performed using two-factor factorial ANOVA and Student's *t*-test, respectively. The other data comparisons were performed using the Mann-Whitney U test.

Results

Effects of PEG-IFN-α2a on Liver Cancer Cell Proliferation *in vitro*

Twenty-four hours after the addition of 4,194 ng/mL of PEG-IFN-α2a, mild increase in the relative viable cell number occurred in 9 cell lines (all cell lines except KYN-2, HAK-1A, HAK-6, and KMCH-1). However, after 72 hours or later, a 10% or more decrease in the cell number occurred in all cell lines (Figure 1A). In HAK-2, HAK-3, and HAK-4, HAK-6, and KMCH-2, proliferation was suppressed up to 72 hours and the cell number reached a plateau or slightly increased thereafter. In the other 8 cell lines, proliferation was suppressed to varying degrees up to 96 hours.

The relative viable cell number was suppressed in 11 cell lines (all cell lines except HAK-1A and KMCH-2) in a dose-dependent manner after the 96 hours-incubation with PEG-IFN-α2a (Figure 1B). In 7 cell lines (HAK-1B, KMCH-1, KIM-1, KYN-1, HAK-6, KYN-3, and KYN-2), the number was suppressed to 50% or less with 4,194 ng/mL of PEG-IFN-α2a, and the 50% inhibitory concentration (IC50) was 253 ng/mL for HAK-1B, 670 ng/mL for KMCH-1, 1,105 ng/mL for KIM-1, 1,128 ng/mL for KYN-1, 1,302 ng/mL for HAK-6, 1,524 ng/mL for KYN-3, and 4,431 ng/mL for KYN-2. No relationship was detected between the histological differentiation level of the original tumor and sensitivity to the anti-proliferative effect of PEG-IFN-α2a.

Seventy-two hours after adding 4,194 ng/mL of PEG-IFN-α2a, 8 cell lines (all cell lines except KYN-3, HAK-1A, HAK-2, HAK-3, and KMCH-2) showed characteristics of apoptosis, e.g., cytoplasmic shrinkage, chromatin condensation, and nuclear fragmentation, in various degrees and in a dose-dependent manner (Figure 2). The appearance of apoptosis was further confirmed in HAK-1B and KIM-1 cells cultured with 10 ng/ml (=2,000 IU/ml) of IFN-α2a or 144 ng/ml (=2,000 IU/ml) of PEG-IFN-α2a by apoptosis detection assay (Table 1). Non-pegylated IFN-α2a induced much more apoptosis than PEG-IFN-α2a.

Effects of PEG-IFN-α2a on HCC Cell Proliferation in Nude Mice

Chronological changes in estimated tumor volume after subcutaneous injection of cultured HAK-1B or KIM-1cells to nude mice are summarized in Figure 3. Dose-dependent suppression of tumor volume was observed in mice receiving PEG-IFN-α2a. In the experiment of HAK-1B tumors, a significant difference in the changes in tumor volume and tumor weight was observed between the Control mice and the mice

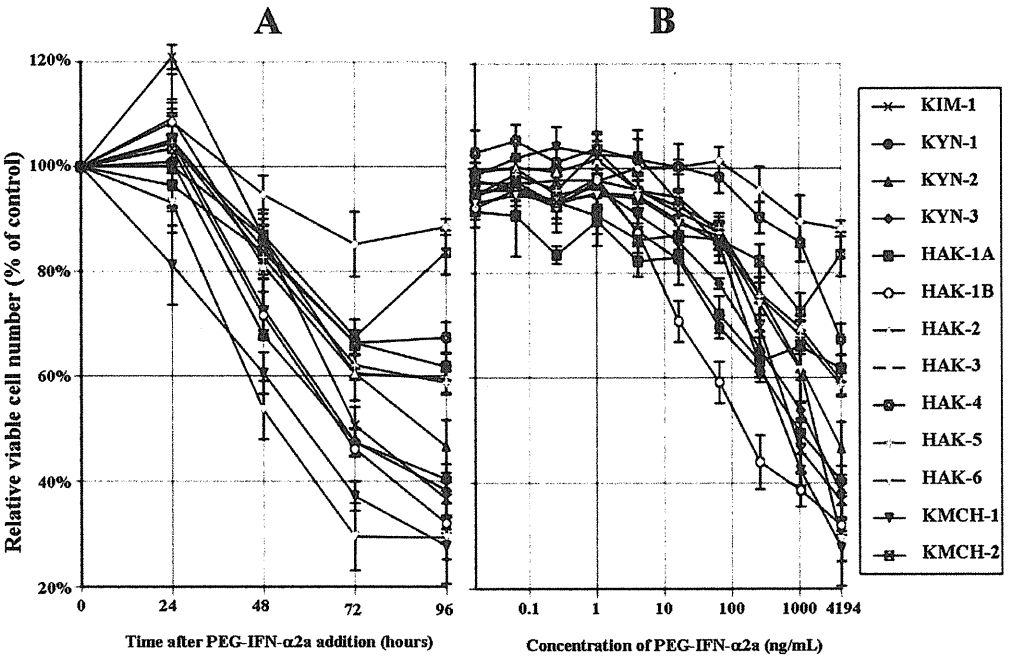

Figure 1. Anti-proliferative effect of PEG-IFN-α2a. (A) Chronological changes in relative viable cell number (% of the control) after adding 4,194 ng/mL of PEG-IFN-α2a. Growth was suppressed with time in 8 cell lines. (B) 96 hours after adding 10 different concentrations of PEG-IFN-α2a. Cell proliferation was suppressed in a dose-dependent manner in 11 cell lines. The suppression was significant ($P < 0.0001$~0.05) in the ranges of 0.016~4,194 ng/mL of PEG-IFN-α2a in HAK-6, 0.256~4,194 ng/mL in KYN-3 and HAK-1A, 4.096~4,194 ng/mL in KIM-1, KYN-1, HAK-1B, HAK-2 and KMCH-2, 16.4~4,194 ng/mL in KYN-2, HAK-5 and KMCH-1, 262~4,194 ng/mL in HAK-4, and at 4,194 ng/mL in HAK-3 (Student *t*-test). Eight samples were used in each experiment (n = 8). The experiment was repeated at least 3 times for each cell line. The figures represent average ± SE of the experiments.

doi: 10.1371/journal.pone.0083195.g001

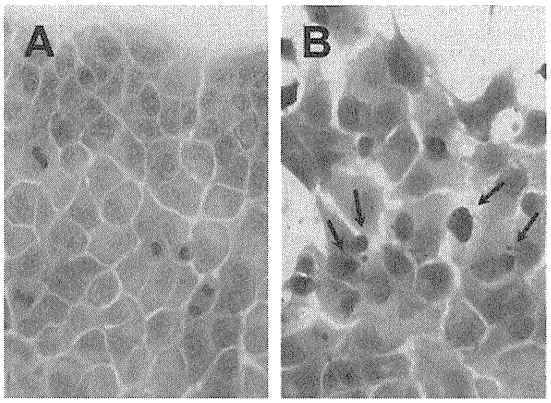

Figure 2. Photomicrograph of HAK-1B cells cultured for 72 hours on a Lab-Tek Chamber slide. (A) Without PEG-IFN-α2a in culture medium. (B) With 4,194 ng/mL of PEG-IFN-α2a in culture medium. Apoptotic cells (short arrows) characterized by cytoplasmic shrinkage, chromatic condensation and nuclear fragmentation were noted (HE staining, X 200).

doi: 10.1371/journal.pone.0083195.g002

Table 1. Quantitative analysis of apoptosis in HAK-1B or KIM-1.

	Annexin V-EGFP apoptotic cells (%)		
Cell line[a]	Control	IFN-α2a	PEG-IFN-α2a
HAK-1B	4.1 ± 0.5[b]	18.5 ± 0.3	10.9 ± 0.5
KIM-1	9.4 ± 0.4	47.0 ± 0.2	29.8 ± 2.1

[a] Cells were cultured with medium alone (Control), IFN-α2a (10 ng/ml=2,000 IU/ml) or PEG-IFN-α2a (144 ng/ml=2,000 IU/ml). [b] Mean ±SE.

doi: 10.1371/journal.pone.0083195.t001

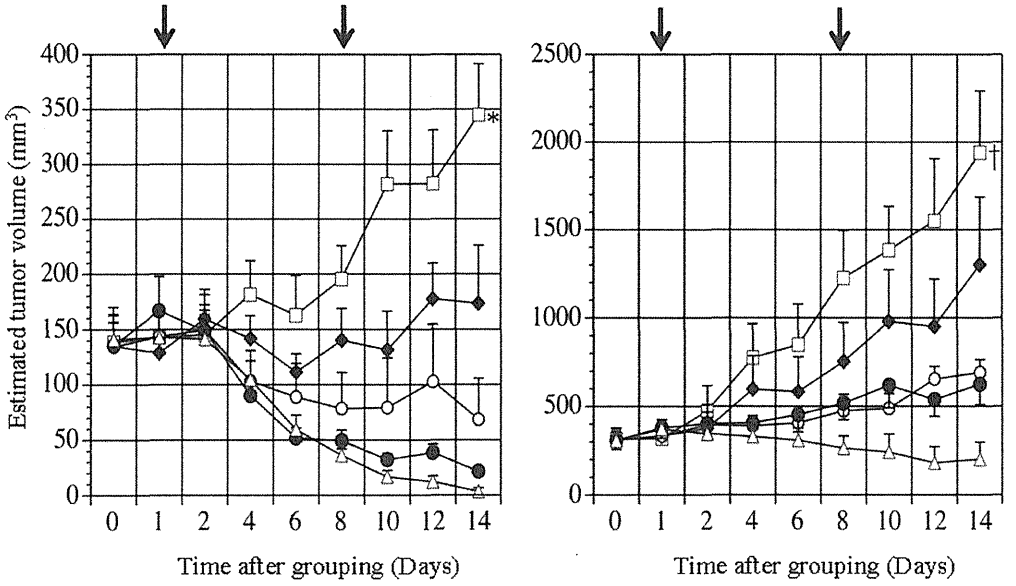

Figure 3. Time-course change in estimated tumor volumes of subcutaneously transplanted HAK-1B (A) or KIM-1 (B) tumors in nude mice in Experiment 1. The mice received a subcutaneous injection of 0.06 (▲), 0.6 (○), 6 (●), or 60 (△) μg of PEG-IFN-α2a, or medium alone (Control) (□), once a week for 2 consecutive weeks. The arrows show the days of injection. The figures represent average ± SE. *$P < 0.0001$, versus the other groups. †$P < 0.01$, versus the other groups.

doi: 10.1371/journal.pone.0083195.g003

that received 0.06, 0.6, 6 or 60 μg of PEG-IFN-α2a ($P < 0.0001$ by two-factor factorial ANOVA; and $P < 0.001$~0.02 by the Mann-Whitney U test, Figure 3A and Table 2). In the experiment of KIM-1 tumors, a significant reduction of tumor volume was also observed with the use of PEG-IFN-α2a ($P < 0.001$ by two-factor factorial ANOVA, Figure 3B). There were significant differences in the actual tumor weight between the Control group and the PEG-IFN-α2a groups, except for the PEG-IFN-α2a (0.06 μg) group (Table 2). The actual tumor weight at the end of the experiment 2 was summarized in Table 3. Subcutaneous injection of 0.6 μg of PEG-IFN-α2a induced the significant reduction of tumor weight, compared with the Control group and the group that received the same international unit of non-pegylated IFN-α2a ($P<0.005$ and $P<0.03$, respectively). In this experiment, there was no significant difference between the Control group and the PEG-IFN-α2a (0.06 μg) group ($P=0.078$).

Histological examination of the HAK-1B tumor specimens stained with HE revealed that the numbers of apoptotic cells in the mice treated with PEG-IFN-α2a (0.06 or 0.6 μg) were significantly higher than that of the Control, and the number increased dose dependently (Figure 4, A and B; Table 4). The incidence of apoptosis in TUNEL-stained sections showed the same tendencies as those obtained in HE-stained sections (Figure 4C and Table 4). Immunohistochemical examination of BrdU uptake in HAK-1B tumors revealed that there was no significant difference in BrdU labeling index between the Control and PEG-IFN-α2a (0.06 or 0.6 μg) groups (Table 4). As for apoptosis, similar findings were observed in experiment 2 in which KIM-1 was used. The group treated with 0.6 μg of PEG-IFN-α2a showed increased number of apoptotic cells than the control group. There was no significant difference between the control and IFN-α2a group. In addition, the group treated with

Table 2. The weight of subcutaneous tumors of HAK-1B or KIM-1 cells in nude mice at killing (Experiment 1).

	Tumor weight (g)	
Treatment group[a]	HAK-1B	KIM-1
Control	0.303 ± 0.05[b, c]	1.050 ± 0.24[e]
PEG-IFN-α2a (0.06 μg)	0.141 ± 0.03[d]	0.725 ± 0.17[f]
PEG-IFN-α2a (0.6 μg)	0.033 ± 0.01	0.439 ± 0.04
PEG-IFN-α2a (6 μg)	0.015 ± 0.01	0.434 ± 0.04
PEG-IFN-α2a (60 μg)	0.0	0.076 ± 0.05

[a] Cultured HAK-1B or KIM-1 cells (1.0 X 10^7) were subcutaneously transplanted into nude mice. Five groups of 8 mice received either phosphate-buffered saline (PBS) (Control) or PBS with the different dosages of PEG-IFN-α2a (0.06–60 μg) once a week. All mice were killed and the tumor weight was measured on the 15th day. [b] Mean ± SE. [c] $P < 0.02$, *versus the PEG-IFN-α2a (0.06 μg) group*; $P < 0.001$, *versus the PEG-IFN-α2a (0.6 μg) group*; $P < 0.001$, *versus the PEG-IFN-α2a (6 μg) group*. [d] $P < 0.02$, versus PEG-IFN-α2a (60 μg). [e] Not significant, versus the PEG-IFN-α2a (0.06 μg) group; $P < 0.03$, versus the PEG-IFN-α2a (0.6 μg) group; $P < 0.05$, versus the PEG-IFN-α2a (6 μg) group; $P < 0.01$, versus the PEG-IFN-α2a (60 μg) group. [f] $P < 0.05$, versus the PEG-IFN-α2a (60 μg) group.

doi: 10.1371/journal.pone.0083195.t002

Table 3. The actual weight and numbers of apoptotic cells of subcutaneous tumors at killing (Experiment 2).

Treatment group[a]	activity of interferon (IU)	Tumor weight (g)	Apoptosis (Number of cells/0.25mm^2)
Control	0 IU	0.726 ± 0.09[b, c]	7.6 ± 0.9[d]
IFN-α2a (0.0042 μg)	840 IU	0.588 ± 0.07[d]	7.9 ± 0.9[g]
IFN-α2a (0.042 μg)	8,400 IU	0.531 ± 0.04[e]	7.6 ± 0.7[h]
PEG-IFN-α2a (0.06 μg)	840 IU	0.493 ± 0.04[f]	8.9 ± 0.9
PEG-IFN-α2a (0.6 μg)	8,400 IU	0.355 ± 0.03	9.7 ± 1.0*

[a] Cultured HAK-1B cells (1.0 X 10^7) were subcutaneously transplanted into nude mice. Five groups of 8 mice received either PBS (Control), PBS with 0.0042 or 0.042 μg of IFN-α2a (840 or 8,400 IU, respectively), or PBS with 0.06 or 0.6 μg of PEG-IFN-α2a (840 or 8,400 IU, respectively). All mice were killed and the tumor weight was measured on the 15th day. The number of apoptotic cells was counted in at least three 0.25 mm^2-areas in each section stained with hematoxylin and eosin, and the average number per area in each group was obtained. [b] Mean ± SE. [c] $P < 0.005$, versus the PEG-IFN-α2a (0.6 μg) group. [d] $P < 0.02$, versus the PEG-IFN-α2a (0.6 μg) group. [e] $P < 0.03$, versus the PEG-IFN-α2a (0.6 μg) group. [f] $P < 0.02$, versus the PEG-IFN-α2a (0.6 μg) group. [g] $P < 0.05$, versus the PEG-IFN-α2a (0.6 μg) group. [h] $P < 0.001$, versus the PEG-IFN-α2a (0.6 μg) group.

doi: 10.1371/journal.pone.0083195.t003

0.6 μg of PEG-IFN-α2a (8,400 IU) showed higher number of apoptotic cells than those with 0.042 μg of IFN-α2a (8,400 IU).

The resected tumor of the PEG-IFN-α2a group showed granulation tissue at the middle of the tumor to various degrees (Figure 5). Arteries that appeared in the granulation tissue were excluded in blood vessel count within tumor. There was no significant difference in the number of blood vessels per unit area within the HAK-1B tumor and the expression of bFGF and IL-8 in the tumors between the PEG-IFN-α2a group and the Control group (Figure 5; Table 5).

Discussion

In the *in vitro* study, we showed that PEG-IFN-α2a inhibit the growth of 8 and 11 out of 13 cell lines in a time- and dose-dependent manner, however, PEG-IFN-α2a was apparently less active on an IC50 basis, compared with either PEG-IFN-α2b or IFN-α2b or consensus IFN-α or BALL-1 lymphoblastoid IFN-α which was tested in the same experimental condition in our previous reports [10,18,21]. For example, IC50 for HAK-1B cells was approximately 253 ng/ml of PEG-IFN-α2a, 13.1 ng/ml of PEG-IFN-α2b, 2.4 ng/ml of IFN-α2b, 0.7 ng/ml of consensus IFN-α and 1.1 ng/ml of BALL-1 lymphoblastoid IFN-α. On the other hand, in the *in vivo* study, s.c. injection of PEG-IFN-α2a once a week showed better antitumor effect on a tumor volume or weight basis, compared with that of non-pegylated IFN-α2a. These results might support our hypothesis that continuous contact with IFNs induces strong *in vivo* antitumor effects, and are not surprising because it was reported that PEG-IFN-α2a showed less active in vitro antiviral activity and but had much more *in vivo* antitumor activity than non-pegylated IFN-α2a [23]. We also showed that PEG-IFN-α2a can inhibit the proliferation of CHC cell lines as well as HCC. In MTT assay, the growth of KMCH-1 was well suppressed although another CHC cell line, KMCH-2 was not. One possible explanation for the different sensitivity between KMCH-1 and KMCH-2 is that the origin of KMCH-1 is CHC, classical type and that of KMCH-2 is CHC with stem-cell features, intermediate-cell subtype according to the latest WHO classification [24]. Such a stem-cell properties of the tumor might be the reason for IFN resistance. Another interesting finding in the *in vitro* study is the discrepancy between the results of MTT assay and apoptosis detection assay. When HAK-1B or KIM-1 was cultured with PEG-IFN-α2a, IC50 for HAK-1B was much lower than that for KIM-1 although HAK-1B showed lower rate of apoptotic cells than KIM-1. These findings suggest that there might be some

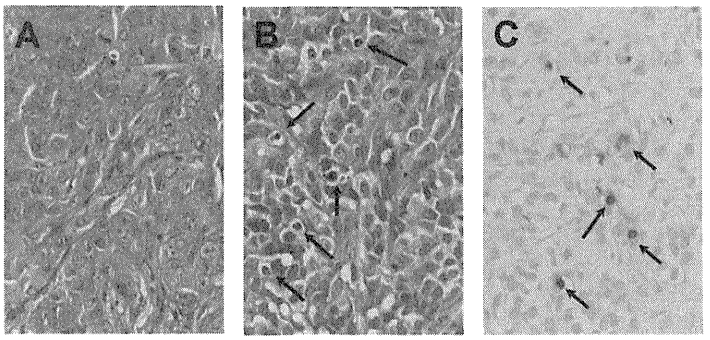

Figure 4. Photomicrograph of subcutaneous human HCC tumor in nude mice that was developed after the injection of HAK-1B cells. (A) A control mouse that received culture medium alone. The tumor shows a compact arrangement of tumor cells and a sinusoid-like structure in the stroma. (B) A mouse that received a s.c. injection of 0.06 μg of PEG-IFN-α2a. There are some apoptotic tumor-cells characterized by shrinkage and eosinophilic change in the cytoplasm, chromatin condensation and/or fragmentation of nuclei (arrows, HE staining, X200). (C) The same tumor as shown in (B). There are some TUNEL-positive cells showing brown nuclei (arrows, stained by the TUNEL technique, X200).

doi: 10.1371/journal.pone.0083195.g004

Table 4. Numbers of apoptotic cells and BrdU-positive cells in human HCC tumors subcutaneously transplanted in nude mice.

	Apoptosis[b] (Number of cells/0.25mm^2)		BrdU Labeling Index[c] (Number of positive cells/0.25mm^2)
Treatment group[a]	HE stain	TUNEL method	
Control	8.4 ± 0.8[d,e]	9.6 ± 1.1[e]	32.3 ± 1.6[f]
PEG-IFN-α2a (0.06 μg)	12.2 ± 1.0	15.4 ± 1.8	27.0 ± 2.6
PEG-IFN-α2a (0.6 μg)	12.4 ± 0.9	16.1 ± 1.5	31.3 ± 6.9

[a] Cultured HAK-1B cells (1.0 X 10^7) were subcutaneously transplanted into nude mice. Five groups of 8 mice received either phosphate-buffered saline (PBS) (Control) or PBS with the different dosages of PEG-IFN-α2a (0.06–60 μg) once a week. Tumors of mice that received 6 or 60 μg of PEG-IFN-α2a could not be used because the tumors were too small to evaluate. All mice were killed on the 15th day. [b] The number of apoptotic cells was counted in at least three 0.25 mm^2-areas in each section stained with hematoxylin and eosin, and the average number per area in each group was obtained. The number of TUNEL-positive cells was also counted in the same manner. [c] The number of BrdU-positive cells was counted in at least three 0.25 mm^2-areas in each section, and the average number per area in each group was obtained as the labeling index. [d] Mean ± SE. [e] $P < 0.02$, versus the other groups. [f] Not significant, versus the other groups.

doi: 10.1371/journal.pone.0083195.t004

mechanisms other than apoptosis, which affect the sensitivity to antitumor effects of PEG-IFN-α2a. We previously reported that both pegylated and non-pegylated IFN-α inhibited the proliferation of cultured HCC cells by inducing the cell-cycle arrest [10,18]. The expression of interferon receptor on tumor cells might be a possible factor related to antitumor effect. For instance, Nagano et al reported that the expression of this type I IFN receptor on HCC tissue might be a useful predictor to find potential responder to INF-α/5-fluorouracil combination therapy [25]. Immunomodulation by IFNs has also been well studied as a factor related to antitumor effect. In this study, we used athymic mice, which lack mature T-cell, and human IFNs. Since IFNs are species-specific [26], we surmise that this immunomodulatory effect is limited in our study, but this should be confirmed in the future study using mouse IFN.

Morphological observation of the subcutaneous tumors of nude mice revealed that s.c. injection of PEG-IFN-α2a induce the significant increase of apoptotic cells compared with Control group. This result in the *in vivo* study is consistent with that in the *in vitro* study showing characteristic changes of apoptosis after adding PEG-IFN-α2a. Although the inhibition of angiogenesis as well as the induction of apoptosis is regarded as one of the biological effects of IFNs, there was no significant difference in the number of artery-like blood vessels of the subcutaneous tumors between the control and treatment groups. There are two possible explanations of this finding. Firstly, PEG-IFN-α2a was less effective for mouse endothelial cells compared with human cancer cells due to the species specificity of human IFNs. Secondly, it might be difficult to visualize the alteration in the number of vessels in order to examine the efficacy of drugs that possess antiangiogenic

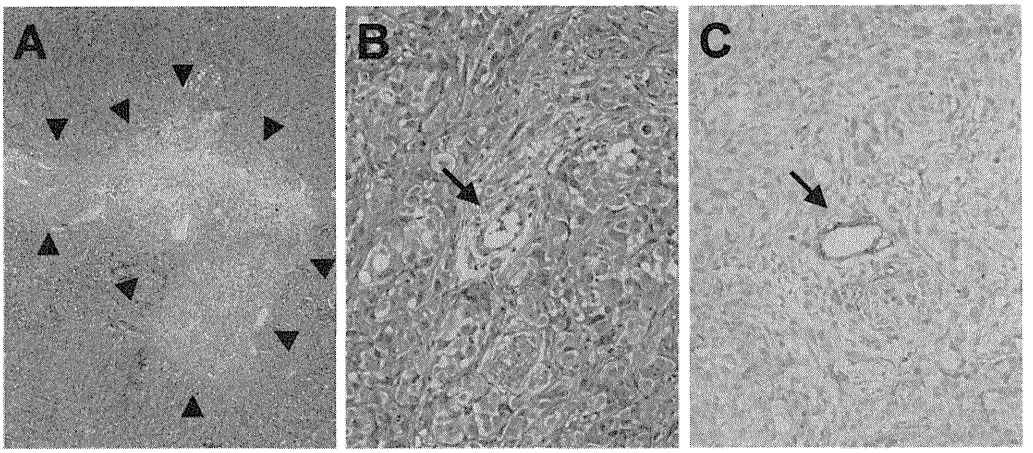

Figure 5. Photomicrograph of resected HAK-1B tumor. (A) Tumor cells are replaced with large granulation tissue at the middle of resected tumor. (arrowheads, HE staining, X20). (B) Artery-like blood vessels in the tumor (arrow, HE staining, X200). (C) Artery-like blood vessel in the tumor (arrow, CD34/α-SMA double-immunostain, X200).
doi: 10.1371/journal.pone.0083195.g005

Table 5. Numbers of artery-like blood vessels, and Enzyme-linked immunosorbent assay (ELISA) of angiogenesis factors in human HCC tumors subcutaneously transplanted in nude mice.

	Artery-like blood vessel[b] (Number of vessels/mm2)	Levels in the tumor lysate[c] (pg/40 μg cellular protein)	
Treatment group[a]	Inside of tumor	bFGF	IL-8
Control	0.104 ± 0.02[d,e]	14.0 ± 1.8[e]	2.8 ± 1.0[e]
PEG-IFN-α2a (0.06 μg)	0.194 ± 0.05	19.8 ± 2.1	4.9 ± 1.3

[a] Cultured HAK-1B cells (1.0 X 10^7) were subcutaneously transplanted into nude mice. Five groups of 8 mice received either phosphate-buffered saline (PBS) (Control) or PBS with the different dosages of PEG-IFN-α2a (0.06–60 μg) once a week. Tumors of mice that received 0.6, 6 or 60 μg of PEG-IFN-α2a could not be used because the tumors were too small to evaluate. All mice were killed on the 15th day. [b] The number of artery-like blood vessels within tumor was counted on each section, and the average number per area in each group was obtained. [c] The expression levels of basic fibroblast growth factor (bFGF) and IL-8 of the resected tumors were measured by ELISA. [d] Mean ± SE. [e]. Not significant, versus the PEG-IFN-α2a (0.06 μg) group.
doi: 10.1371/journal.pone.0083195.t005

activity. Hlatky et al explained in their review article that the reason is that the tightness of the coupling between vessel drop-out and tumor-cell drop-out after the treatment is different [27]. We had observed similar findings in our previous report in which human HCC tumors subcutaneously transplanted in nude mice showed much apoptosis in either PEG-IFN-α2b or IFN-α2b treatment group compared with the Control group, but no significant difference in the number of blood vessels [10]. Kojiro et al also showed that s.c. injection of BALL-1 lymphoblastoid IFN-α increase the number of artery-like blood vessels and the protein expression of bFGF within HCC xenograft tumors in spite of the significant decrease of actual tumor weight [28]. In contrast, Dinney et al showed that IFN-α2a decreases the blood vessel density and the expression of bFGF in orthotopic xenograft model of bladder tumor [29]. The reason for these contrary findings remains unclear and further evaluation with caution is needed by using different doses and types of IFNs and different cell lines, not only in subcutaneous tumor model but also in orthotopic model.

The association between IFN therapy and occurrence or recurrence of HCC has been investigated in some reports. HALT-C trial group showed in their randomized control trial in a large cohort that long-term PEG-IFN-α2a therapy does not reduce the incidence of HCC among patients with chronic HCV infection who have previously failed to achieve a sustained virologic response to therapy [30]. Among only patients with cirrhosis, long-term PEG-IFN-α2a therapy reduced a risk of HCC after a long-time observation [31]. EPIC study group also showed long-term PEG-IFN-α2b therapy does not prevent HCC [32]. On the other hand, Nishiguchi et al reported that long-term IFN-α therapy after curative resection of HCV-related HCC prolongs the survival rate, although preventive effect of intrahepatic recurrence was marginal [33]. Sakaguchi et al also showed that among patients who underwent radical

radiofrequency therapy for HCV-related HCC, long-term IFN-α2b therapy reduced the recurrent rate of HCC [4]. These reports with conflicting results may be suggesting that IFN therapy is effective only after the initial curative treatment of HCV-related HCC. In addition, there are several reports that support that IFN therapy prevents the development of HCC among patients with chronic HBV infection or those underwent curative resection of HBV-related HCC [5,7]. Thus the chemopreventive effect of IFNs against HCC are still controversial, and mechanisms behind that remain unclear. Antiviral effect against HBV and HCV, which are risk factors for HCC, and immunomodulatory effect of IFNs are regarded as main mechanisms. Another possible mechanism is that IFNs may suppress the growth of clinically undetectable HCC due to their direct antitumor effect. Our finding in the current study provide the evidence that PEG-IFN-α2a possesses the direct antitumor effect against HCC.

In conclusion, we demonstrated antitumor effect of PEG-IFN-α2a for human liver cancer cells *in vitro* and *in vivo* and our results suggest that longer contact to IFNs may induce stronger antitumor effect in body. PEG-IFN-α2a might be a possible treatment option for HCC as well as chronic viral hepatitis. Further studies are needed from both molecular and clinical view points in order to find out particular patient group those respond to this therapy.

Acknowledgements

We thank Ms. Akemi Fujiyoshi for her assistance in our experiments.

Author Contributions

Conceived and designed the experiments: HK JA SO ON HY. Performed the experiments: HK JA SO SS MY MN KU KU TK KT YU ON HY. Analyzed the data: HK JA SO SS MY MN KU KU TK KT YU ON HY. Contributed reagents/materials/analysis tools: HK JA SO SS MY MN KU KU TK KT YU ON HY. Wrote the manuscript: HK JA SO ON HY.

References

1. Pestka S, Langer JA, Zoon KC, Samuel CE (1987) Interferons and their actions. Annu Rev Biochem 56: 727–777. doi:10.1146/annurev.bi.56.070187.003455. PubMed: 2441659.
2. Jonasch E, Haluska FG (2001) Interferon in oncological practice: review of interferon biology, clinical applications, and toxicities. Oncologist 6: 34–55. doi:10.1634/theoncologist.6-1-34. PubMed: 11161227.
3. Lai CL, Lau JY, Wu PC, Ngan H, Chung HT et al. (1993) Recombinant interferon-alpha in inoperable hepatocellular carcinoma: a randomized controlled trial. Hepatology. 17: 389-394. doi:10.1002/hep.1840170307. PubMed: 8383088.
4. Sakaguchi Y, Kudo M, Fukunaga T, Minami Y, Chung H et al. (2005) Low-dose, long-term, intermittent interferon-alpha-2b therapy after radical treatment by radiofrequency ablation delays clinical recurrence in patients with hepatitis C virus-related hepatocellular carcinoma. Intervirology 48: 64–70. doi:10.1159/000082097. PubMed: 15785092.
5. Miyake Y, Kobashi H, Yamamoto K (2009) Meta-analysis: the effect of interferon on development of hepatocellular carcinoma in patients with chronic hepatitis B virus infection. J Gastroenterol 44: 470–475. doi: 10.1007/s00535-009-0024-z. PubMed: 19308310.
6. Miyake Y, Iwasaki Y, Yamamoto K (2010) Meta-analysis: reduced incidence of hepatocellular carcinoma in patients not responding to interferon therapy of chronic hepatitis C. Int J Cancer 127: 989–996. PubMed: 19957327.
7. Qu LS, Jin F, Huang XW, Shen XZ (2010) Interferon-α therapy after curative resection prevents early recurrence and improves survival in patients with hepatitis B virus-related hepatocellular carcinoma. J Surg Oncol 102: 796–801. doi:10.1002/jso.21741. PubMed: 20886584.
8. Manns MP, McHutchison JG, Gordon SC, Rustgi VK, Shiffman M et al. (2001) Peginterferon alfa-2b plus ribavirin compared with interferon alfa-2b plus ribavirin for initial treatment of chronic hepatitis C: a randomised trial. Lancet 358: 958–965. doi:10.1016/S0140-6736(01)06102-5. PubMed: 11583749.
9. Fried MW, Shiffman ML, Reddy KR, Smith C, Marinos G et al. (2002) Peginterferon alfa-2a plus ribavirin for chronic hepatitis C virus infection. N Engl J Med 347: 975–982. doi:10.1056/NEJMoa020047. PubMed: 12324553.
10. Yano H, Ogasawara S, Momosaki S, Akiba J, Kojiro S et al. (2006) Growth inhibitory effects of pegylated IFN alpha-2b on human liver cancer cells *in vitro* and *in vivo*. Liver Int 26: 964–975. doi:10.1111/j.1478-3231.2006.01321.x. PubMed: 16953837.
11. Utsunomiya I, Iemura A, Yano H, Akiba J, Kojiro M (1999) Establishment and characterization of a new human hepatocellular carcinoma cell line, HAK-3, and its response to growth factors. Int J Oncol 15: 669–675. PubMed: 10493947.
12. Murakami T (1984) Establishment and characterization of human hepatoma cell line (KIM-1). Acta Hepatol Jpn 25: 532–539. doi: 10.2957/kanzo.25.532.
13. Murakami T, Maruiwa M, Fukuda K, Kojiro M, Tanaka M, et al. (1988) Characterization of a new human hepatoma cell line (KYN-3) derived from the ascites of the hepatoma patient [Abstract]. Jpn J Cancer Res 292 Proceedings of the Japanese Cancer Association
14. Murakami T, Yano H, Maruiwa M, Sugihara S, Kojiro M (1987) Establishment and characterization of a human combined hepatocholangiocarcinoma cell line and its heterologous transplantation in nude mice. Hepatology 7: 551–556. doi:10.1002/hep.1840070322. PubMed: 3032760.
15. Haramaki M, Yano H, Iemura A, Momosaki S, Ogasawara S et al. (1997) A new human hepatocellular carcinoma cell line (HAK-2) forms various structures in collagen gel matrices. Hum Cell 10: 183–192. PubMed: 9436038.
16. Yano H, Iemura A, Fukuda K, Mizoguchi A, Haramaki M et al. (1993) Establishment of two distinct human hepatocellular carcinoma cell lines from a single nodule showing clonal dedifferentiation of cancer cells. Hepatology 18: 320–327. doi:10.1016/0270-9139(93)92802-7. PubMed: 8393423.
17. Yano H, Iemura A, Haramaki M, Momosaki S, Ogasawara S et al. (1996) A human combined hepatocellular and cholangiocarcinoma cell line (KMCH-2) that shows the features of hepatocellular carcinoma or cholangiocarcinoma under different growth conditions. J Hepatol 24: 413–422. doi:10.1016/S0168-8278(96)80161-9. PubMed: 8738727.
18. Yano H, Iemura A, Haramaki M, Ogasawara S, Takayama A et al. (1999) Interferon alfa receptor expression and growth inhibition by interferon alfa in human liver cancer cell lines. Hepatology 29: 1708–1717. doi:10.1002/hep.510290624. PubMed: 10347112.
19. Yano H, Kojiro M, Nakashima T (1986) A new human hepatocellular carcinoma cell line (KYN-1) with a transformation to adenocarcinoma. In Vitro Cell Dev Biol 22: 637–646. doi:10.1007/BF02623477. PubMed: 2430933.
20. Yano H, Maruiwa M, Murakami T, Fukuda K, Ito Y et al. (1988) A new human pleomorphic hepatocellular carcinoma cell line, KYN-2. Acta Pathol Jpn 38: 953–966. PubMed: 2847482.
21. Hisaka T, Yano H, Ogasawara S, Momosaki S, Nishida N et al. (2004) Interferon-αCon1 suppresses proliferation of liver cancer cell lines *in vitro* and *in vivo*. J Hepatol 41: 782–789. doi:10.1016/j.jhep.2004.07.012. PubMed: 15519651.
22. Takemoto Y, Yano H, Momosaki S, Ogasawara S, Nishida N et al. (2004) Antiproliferative effects of interferon-alphaCon1 on ovarian clear cell adenocarcinoma *in vitro* and *in vivo*. Clin Cancer Res 10: 7418–7426. doi:10.1158/1078-0432.CCR-04-0279. PubMed: 15534119.
23. Bailon P, Palleroni A, Schaffer CA, Spence CL, Fung WJ et al. (2001) Rational design of a potent, long-lasting form of interferon: a 40 kDa branched polyethylene glycol-conjugated interferon alpha-2a for the treatment of hepatitis C. Bioconjug Chem 12: 195-202. doi:10.1021/bc000082g. PubMed: 11312680.

24. Bosman FT, Carneiro F, Hruban RH, Theise ND (2010) WHO Classification of Tumours of the Digestive System (4th Revised edition). Lyon, France, IARC Press. pp. 225-227.
25. Nagano H, Miyamoto A, Wada H, Ota H, Marubashi S et al. (2007) Interferon-alpha and 5-fluorouracil combination therapy after palliative hepatic resection in patients with advanced hepatocellular carcinoma, portal venous tumor thrombus in the major trunk, and multiple nodules. Cancer 110: 2493–2501. doi:10.1002/cncr.23033. PubMed: 17941012.
26. Gillespie G, Carter WA (1981-1982) Species specificity of interferon. Tex Rep Biol Med 41: 37-42. PubMed: 6184826.
27. Hlatky L, Hahnfeldt P, Folkman J (2002) Clinical application of antiangiogenic therapy: microvessel density, what it does and doesn't tell us. J Natl Cancer Inst 94: 883-893. doi:10.1093/jnci/94.12.883. PubMed: 12072542.
28. Kojiro S, Yano H, Ogasawara S, Momosaki S, Takemoto Y et al. (2006) Antiproliferative effects of 5-fluorouracil and interferon-alpha in combination on a hepatocellular carcinoma cell line *in vitro* and *in vivo*. J Gastroenterol Hepatol 21: 129–137. doi:10.1111/j.1440-1746.2005.04154.x. PubMed: 16706824.
29. Dinney CP, Bielenberg DR, Perrotte P, Reich R, Eve BY et al. (1998) Inhibition of basic fibroblast growth factor expression, angiogenesis, and growth of human bladder carcinoma in mice by systemic interferon-alpha administration. Cancer Res 58: 808–814. PubMed: 9485039.
30. Di Bisceglie AM, Shiffman ML, Everson GT, Lindsay KL, Everhart JE et al. (2008) Prolonged therapy of advanced chronic hepatitis C with low-dose peginterferon. N Engl J Med 359: 2429–2441. doi:10.1056/NEJMoa0707615. PubMed: 19052125.
31. Lok AS, Everhart JE, Wright EC, Di Bisceglie AM, Kim HY et al. (2011) Maintenance peginterferon therapy and other factors associated with hepatocellular carcinoma in patients with advanced hepatitis C. Gastroenterology 140: 840–849. doi:10.1053/j.gastro.2010.11.050. PubMed: 21129375.
32. Bruix J, Poynard T, Colombo M, Schiff E, Burak K et al. (2011) Maintenance therapy with peginterferon alfa-2b does not prevent hepatocellular carcinoma in cirrhotic patients with chronic hepatitis C. Gastroenterology 140: 1990–1999. doi:10.1053/j.gastro.2011.03.010. PubMed: 21419770.
33. Nishiguchi S, Tamori A, Kubo S (2005) Effect of long-term postoperative interferon therapy on intrahepatic recurrence and survival rate after resection of hepatitis C virus-related hepatocellular carcinoma. Intervirology 48: 71–75. doi:10.1159/000082098. PubMed: 15785093.

Hepatology Research

Hepatology Research 2013 doi: 10.1111/hepr.12219

Original Article

Pathological characteristics of patients who develop hepatocellular carcinoma with negative results of both serous hepatitis B surface antigen and hepatitis C virus antibody

Reiichiro Kondo,[1,4,5] Osamu Nakashima,[6] Michio Sata,[2] Fumio Imazeki,[7] Osamu Yokosuka,[7] Ken Tanikawa,[5] Masayoshi Kage,[3,4,5] Hirohisa Yano[1] and The Liver Cancer Study Group of Kyushu

[1]Department of Pathology, [2]Division of Gastroenterology, Department of Medicine, [3]Research Center for Innovative Cancer Therapy, Kurume University School of Medicine, [4]Cancer Center, [5]Department of Diagnostic Pathology, [6]Department of Clinical Laboratory Medicine, Kurume University Hospital, Kurume, and [7]Department of Medicine and Clinical Oncology, Graduate School of Medicine, Chiba University, Chiba, Japan

Aim: We tried to characterize the pathological features of patients who developed hepatocellular carcinoma (HCC) with the negative results of both serous hepatitis B surface antigen and hepatitis C virus antibody (non-B, non-C).

Methods: In a multicenter study in Kyushu, Japan, we studied the histopathological characteristics of non-cancerous liver tissues in 129 patients (103 men and 26 women) with non-B, non-C HCC. The histological liver damage was evaluated for fibrosis (stage) and inflammation (grade) according to the Ludwig classification of chronic hepatitis. In addition, we examined the hepatitis B virus (HBV) genome in serum samples and liver tissues of 20 patients with non-B, non-C HCC.

Results: Positivity of serum hepatitis B core (HBc) antibody, alcohol abuse, diabetes and non-alcoholic steatohepatitis were present in 61 (47%), 76 (59%), 57 (44%) and eight (6%) patients, respectively. The degree of fibrosis was mild (stage 1.6 ± 1.2). The stage of patients with neither serum HBc antibody nor alcohol abuse was significantly lower than the stage of patients with HBc antibody and no alcohol abuse ($P < 0.05$). HBV genome was detected in 15 cancerous tissues (75%) and 16 non-cancerous liver tissues (80%) in 20 patients with non-B, non-C HCC. Only three of the 20 patients were positive for serum HBc antibody.

Conclusion: Non-B, non-C patients appear to develop HCC at a low stage of fibrosis. Occult hepatitis B virus infection is the major risk factor for HCC of non-B, non-C patients in Kyushu, Japan.

Key words: diabetes mellitus, hepatocellular carcinoma, large liver cell change, non-alcoholic steatohepatitis, non-B non-C, occult hepatitis B infection

INTRODUCTION

HEPATOCELLULAR CARCINOMA (HCC) is the fifth most common cancer worldwide.[1–3] HCC mostly occurs within an established background of chronic liver disease and cirrhosis. Although the risk factors for HCC, including infection with hepatitis B virus (HBV) and hepatitis C virus (HCV), are well defined,[4–6] some patients with HCC in Japan have no confirmed chronic viral hepatitis, and the percentage of these patients is reportedly much higher in Western countries.[7–9]

Hepatocellular carcinoma cases without chronic viral hepatitis include patients who suffer from other chronic liver diseases predisposing to HCC, such as alcoholic liver disease,[9] hemochromatosis,[10] Budd–Chiari syndrome[11] and non-alcoholic fatty liver disease (NAFLD)/non-alcoholic steatohepatitis (NASH).[12,13] In addition, there is a subpopulation of patients with HCC that develops from normal liver or liver tissue damaged from

Correspondence: Dr Reiichiro Kondo, Department of Pathology, Kurume University School of Medicine, 67 Asahi-machi, Kurume, Fukuoka 830-0011, Japan. Email: kondou_reiichirou@kurume-u.ac.jp
Conflict of interest: The authors declare that they have no conflict of interest.
Received 9 April 2013; revision 18 July 2013; accepted 6 August 2013.

an unknown cause at a constant rate. The incidence and risk factors for HCC in patients without chronic viral hepatitis are not yet clear.

The Liver Cancer Study Group of Kyushu (LCSK) established a working group for the multicenter study to investigate the carcinogenesis of HCC without chronic viral hepatitis. The aim of the study described in the present paper was to clarify the pathological characteristics in non-cancerous liver tissues of patients who developed HCC with the negative results of both serous hepatitis B surface (HBs) antigen and HCV antibody (non-B, non-C) to investigate the carcinogenesis of HCC without chronic viral hepatitis.

METHODS

Tissues

WE STUDIED THE histopathological characteristics of 129 patients with non-B, non-C HCC between 1996 and 2006 with the LCSK and their affiliated hospital in the northern area of Kyushu, Japan. Patients with co-existing liver disease diagnosed by clinical and histological examination, such as autoimmune hepatitis, primary biliary cirrhosis, Budd–Chiari syndrome, hemochromatosis, Wilson disease and *Schistosomiasis japonica*, were excluded. Non-cancerous liver tissues were obtained by percutaneous biopsy or surgical operation (percutaneous biopsy, 65 patients; surgical operation, 64 patients).

In addition, we investigated HBV DNA in cryopreserved serum samples, HCC tissues and non-cancerous liver tissues that were obtained from 20 patients with non-B, non-C HCC in Kurume University Hospital in the period between 1997 and 2008.

This study was performed with informed consent obtained from patients for the use of their liver tissues and serum samples in the investigation and was approved by the ethical committee of Kurume University (approval ID no. 10004).

Histopathological examination of non-cancerous liver tissues

Each tissue was fixed with 10% formalin, embedded in paraffin, cut into 5-μm sections, and then used for histological analyses. The specimens were stained with hematoxylin–eosin and examined under a light microscope.

The histological liver damage of these specimens was evaluated for fibrosis and inflammation according to the Ludwig classification of chronic hepatitis.[14] The severity of fibrosis (stage of disease) was classified as none (stage 0), mild (portal fibrosis, stage 1), moderate (periportal fibrosis, stage 2), severe (bridging fibrosis with lobar distortion, stage 3) and cirrhosis (stage 4), and the inflammatory activity (grade of disease activity) was classified as none (grade 0), minimal (grade 1), mild (grade 2), moderate (grade 3) or severe (grade 4). In addition, the pathological features of hepatocytes, such as fatty change, ballooning and large liver cell change (LCC, Fig. 1), were evaluated.

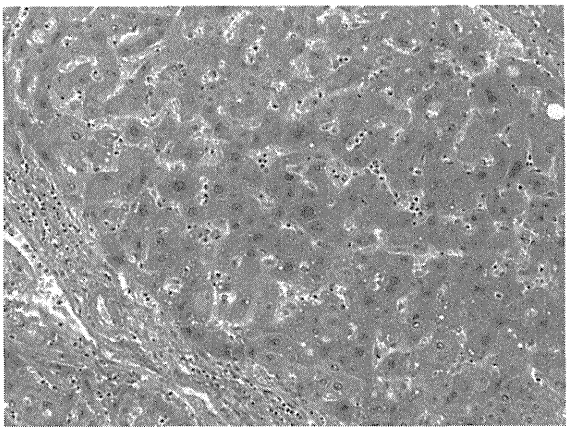

Figure 1 Microscopic findings (Large liver cell change). Large liver cell change is recognized as foci of cellular enlargement and nuclear pleomorphism, hyperchromasia and multinucleation (stained with hematoxylin and eosin, ×200).

Histopathological diagnosis and classification were performed by two pathologists (O. N. and M. K.).

Nucleic acid extraction from serum samples

Total nucleic acid was extracted from 300 μL of plasma using a commercially available kit (High Pure Viral Nucleic Acid Kit; Roche, Mannheim, Germany) according to the manufacturer's instructions. The extracted nucleic acid was eluted in 25 μL of elution buffer.

Nucleic acid extraction from liver tissues

The QIAamp DNA micro kit (QIAGEN, Hilden, Germany) was used to extract the nucleic acid from liver tissues (<10 mg) according to the manufacturer's instructions, with few changes. The DNA was eluted in 60 μL of AE buffer.

Quantification of HBV DNA (S, X, C)

Hepatitis B virus DNA was analyzed for the region of HBs, hepatitis B core (HBc), and hepatitis B x (HBx) by

Table 1 Nucleotide positions and sequences of TaqMan polymerase chain reaction primers and probes

S region	5′–3′	
Sense	TGTACAAAACCTTCGGACGGAAA	442–464
Antisense	TGCGAAAGCCCAGGATGATG	485–504
Probe	CTGCACTTGTATTCCC	465–480
Core region		
Sense	ACTGTGGTTTCACATTTCCTGTCTT	2072–2096
Antisense	GGCATTTGGTGGTCTGTAAGC	2163–2183
Probe	CCACACTCCAAAAGAC	2132–2147
X region		
Sense	CTACTGTTCAAGCCTCCAAGCT	1729–1750
Antisense	GCTCCAAATTCTTTATACGGGTCAATG	1778–1804
Probe	AAGCCACCCAAGGCAC	1751–1766

TaqMan real-time polymerase chain reaction (PCR) according to the manufacture's guidelines (Taqman Fast Universal PCR Master Mix; Applied Biosystems, Foster City, CA, USA). The oligonucleotide primers and probes that were optimized to adr of HBV subtype and specific for S, X and C region sequences, are summarized in Table 1. Plasmid pBRHBadr72 (full-length HBV DNA) was used as an internal standard in the quantitative real-time detection PCR. We used 8 μL nucleic acid from serum in our study for better sensitivity. The limit of sensitivity of our TaqMan real-time PCR methods ranged from 5 copies/well. The detection limit of our tests was 52 copies/mL. For quantification of HBV DNA from liver tissue, we used 3 μL nucleic acid, and a single copy housekeeping gene present in human, β-actin was assayed on the same sample. This was performed to estimate the number of cells presented in each PCR reaction. Serial dilutions of genomic DNA were used as standards to quantitate β-actin DNA from liver biopsies (TaqMan Beta-actin Detection Reagents; Applied Biosystems).

Enzymatic treatment with plasmid-safe adenosine triphosphate (ATP)-dependent DNase for detection of cccDNA

DNA extracted from liver tissue (<10 mg) was diluted to 60 μL in AE buffer. A 40-μL aliquot was put aside for detection of RC DNA (X, S, C regions) and β-actin DNA. The remaining 20 μL was digested with 25 units of Plasmid-Safe ATP-dependent DNase (Epicentre Technologies, Madison, WI, USA) for 30 min at 37°C in the presence of 10 × reaction buffer 5 μL, 25 mM ATP 2 μL, Plasmid-Safe DNase 1 μL and deionized distilled water 22 μL. Then, the reaction was inactivated by incubation at 70°C for 30 min. The mixture was purified using a QIAquick PCR Purification Kit (QIAGEN) and diluted by 40 μL EB buffer.

Quantification of HBV cccDNA

Hepatitis B virus cccDNA was tested using c-sel primers and probes as shown in Figure 2. We used 5 μL HBV cccDNA in the TaqMan real-time PCR. The internal standard was plasmid pBRHBadr72.

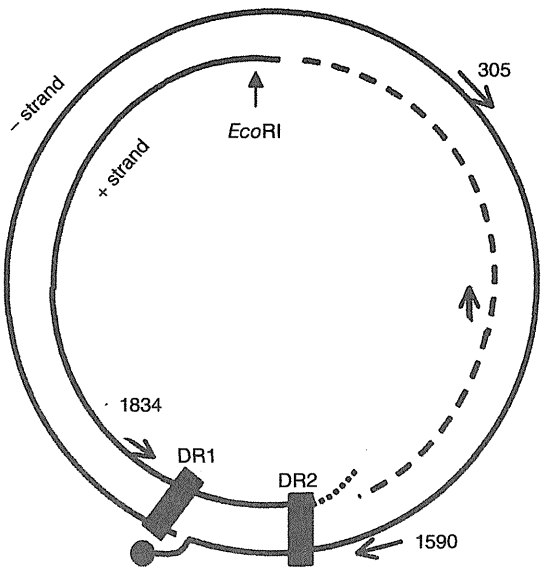

Figure 2 Quantification of HBV cccDNA. HBV cccDNA was tested using c-sel primers and probes. We used 5 μl HBV cccDNA in the Taqman real-time PCR. The internal standard was Plasmid pBRHBadr72.

Table 2 Clinical backgrounds of 129 patients examined by the LCSK

	AL (+)		AL (−)		Total
HBc (+)	40		21		61
	DM (+)	DM (−)	DM (+)	DM (−)	
	M: 15	M: 23	M: 4 (NASH: 1)	M: 8 (NASH: 1)	
	F: 1	F: 1	F: 3 (NASH: 1)	F: 6 (NASH: 1)	
	(A)	(B)	(C)	(D)	
HBc (−)	36		32		68
	DM (+)	DM (−)	DM (+)	DM (−)	
	M: 17	M: 18	M: 9	M: 9	
	F: 0	F: 1	F: 8 (NASH: 3)	F: 6 (NASH: 1)	
	(E)	(F)	(G)	(H)	
Total	76		53		129

(A) Stage 2.1 ± 1.4, grade 2.4 ± 1.2.
(B) Stage 1.8 ± 1.5, grade 1.9 ± 1.7.
(C) Stage 1.9 ± 1.1, grade 1.7 ± 1.4.
(D) Stage 1.8 ± 1.2, grade 2.2 ± 1.7.
(E) Stage 1.8 ± 1.1, grade 2.1 ± 1.2.
(F) Stage 1.3 ± 1.2, grade 1.9 ± 1.1.
(G) Stage 1.4 ± 1.3, grade 2.0 ± 1.4.
(H) Stage 1.0 ± 0.8, grade 1.4 ± 1.0.
Data are expressed as the mean ± standard deviation.
AL, alcohol abuse; DM, diabetes mellitus; F, female; HBc, serum HBc antibody; M, male; NASH, non-alcoholic steatohepatitis.

Statistical analysis

Arithmetic means and standard deviation (SD) of our data were calculated using a JMP software package (version 10.0; SAS Institute, Cary, NC, USA). All data are expressed as the mean ± SD, and *P*-values less than 5% were considered significant.

RESULTS

Clinical background

IN 129 PATIENTS with non-B, non-C HCC examined by the LCSK, there were 103 men and 26 women. The mean age of the men was 68 ± 10 years and the women 70 ± 11 years. Sixty-one patients (47%) were serum HBc antibody positive. Seventy-six patients (59%) abused alcohol (daily intake >60 g of ethanol for men, >40 g for women). Fifty-seven patients (44%) had diabetes mellitus. Most female patients (14 patients) had neither serum HBc antibody nor alcohol abuse (Table 2).

Clinical background and histological findings

Liver fibrosis and inflammation

Non-cancerous liver tissues of 129 patients with non-B, non-C HCC examined by the LCSK showed mild fibrosis and inflammation (grade 2.0 ± 1.4, stage 1.6 ± 1.2). The stage of patients with neither serum HBc antibody nor alcohol abuse was significantly lower than the stage of patients with HBc antibody and alcohol abuse (1.2 ± 1.1 vs 1.9 ± 1.4, $P < 0.03$), and the stage of patients with HBc antibody and no alcohol abuse (1.2 ± 1.1 vs 1.8 ± 1.1, $P < 0.05$) (Table 3). Patients with neither serum HBc antibody, alcohol abuse nor diabetes mellitus were of the lowest grade and stage in patients

Table 3 Clinical backgrounds and histological findings of 129 patients examined by the LCSK

	AL (+)	AL (−)	Total
HBc (+)	40	21	61
	Stage 1.9 ± 1.4	Stage 1.8 ± 1.1	
	Grade 2.1 ± 1.5	Grade 2.0 ± 1.6	
	**	*	
HBc (−)	36	32	68
	Stage 1.6 ± 1.2	Stage 1.2 ± 1.1	
	Grade 2.0 ± 1.6	Grade 1.7 ± 1.2	
Total	76	53	129

Data are expressed as the mean ± standard deviation.
*$P < 0.05$, **$P < 0.03$.
AL, alcohol abuse; HBc, serum HBc antibody; LCSK, Liver Cancer Study Group of Kyushu.

Table 4 Summary of histopathological findings in non-alcoholic patients examined by the LCSK

	Hepatic steatosis	Hepatocellular ballooning	Mallory–Denk body	Lipogranuloma	NASH
HBc (–), DM (–), $n = 15$	6	2	1	1	1
HBc (+), DM (–), $n = 14$	4	5	2	1	2
HBc (–), DM (+), $n = 17$	12	4	3	3	3
HBc (+), DM (+), $n = 7$	6	4	1	2	2

DM, diabetes mellitus; HBc, serum HBc antibody; LCSK, Liver Cancer Study Group of Kyushu; NASH, non-alcoholic steatohepatitis.

examined by the LCSK (stage 1.0 ± 0.8, grade 1.4 ± 1.0; Table 2).

Pathological features of hepatocytes

Non-cancerous liver tissues of 129 patients with non-B, non-C HCC examined by the LCSK showed various pathological features. In 53 patients without alcohol abuse, eight patients were identified as having NASH. There were six female patients of the eight patients with NASH (Table 2). NAFLD was present in 28 patients of the 53 non-alcoholic patients. Of 28 patients with NAFLD, diabetes mellitus was present in 18 (64%) patients (Table 4). LCC was observed in 52 of the 61 patients (85%) with serum HBc antibody, and 44 of the 68 patients (65%) without serum HBc antibody (Fig. 3).

HBV DNA in serum samples and liver tissues

In cryopreserved serum samples, HCC tissues and non-cancerous liver tissues obtained from 20 patients with non-B, non-C HCC, HBV DNA was detected in one serum sample (5%), 15 HCC tissues (75%) and 16 non-cancerous liver tissues (80%) (Table 5). In only two patients, both HCC tissues and non-cancerous liver tissues were negative for HBV DNA detection. In addition, only three of the 20 patients were positive for serum HBc antibody.

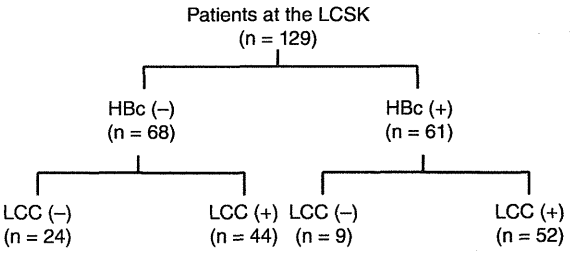

Figure 3 Large liver cell change of 129 patients examined by the Liver Cancer Study Group of Kyushu. There are 96 patients (74%) with large liver cell change (LCC) in 129 patients with non-B, non-C hepatocellular carcinoma. Large liver cell change is observed in 52 of the 61 patients (85%) with serum hepatitis B core (HBc) antibody, and 44/68 patients (65%) without serum HBc antibody.

DISCUSSION

RECENTLY, THE AVAILABILITY of vaccines for HBV has decreased the proportion of patients with HBs antigen by preventing mother-to-infant infection.[15] Antiviral therapy in patients with HCV may prevent carcinogenesis.[16,17] The incidence of HCC associated with HBV or HCV is thus forecast to decrease in Japan, whereas HCC without hepatitis virus infection will remain.[7,18] In this study, we demonstrated the pathological characteristics in non-cancerous liver tissues of patients with non-B, non-C HCC.

Patients with non-B, non-C HCC have various clinical backgrounds, such as serum HBc antibody, alcohol abuse and diabetes mellitus. Abe *et al.*[8] reported 64 patients with non-B, non-C HCC in Tokyo, Japan. Positivity of serum HBc antibody, alcohol abuse and diabetes mellitus was present in 34 (53.1%), 46 (71.9%) and 29 (45.3%) patients, respectively. Yano *et al.*[19] reported 22 patients with non-B, non-C HCC in Saga, Kyushu, Japan. Positivity of serum HBc antibody was present in 16 (72.7%) patients. In this study, we studied 129 patients with non-B, non-C HCC in the northern area of Kyushu, Japan. Positivity of serum HBc antibody, alcohol abuse and diabetes mellitus was present in 61 (47%), 76 (59%) and 57 (44%) patients, respectively. We considered that there were regional differences with respect to the frequency of the non-B, non-C HCC development risk factors, such as positivity of serum HBc antibody, alcohol abuse and diabetes mellitus.

Hepatitis C virus infection, HBV infection, alcohol abuse and NASH are the main causes of liver fibrosis.[20] In this study, non-cancerous liver tissues of patients with neither serum HBc antibody, alcohol abuse nor